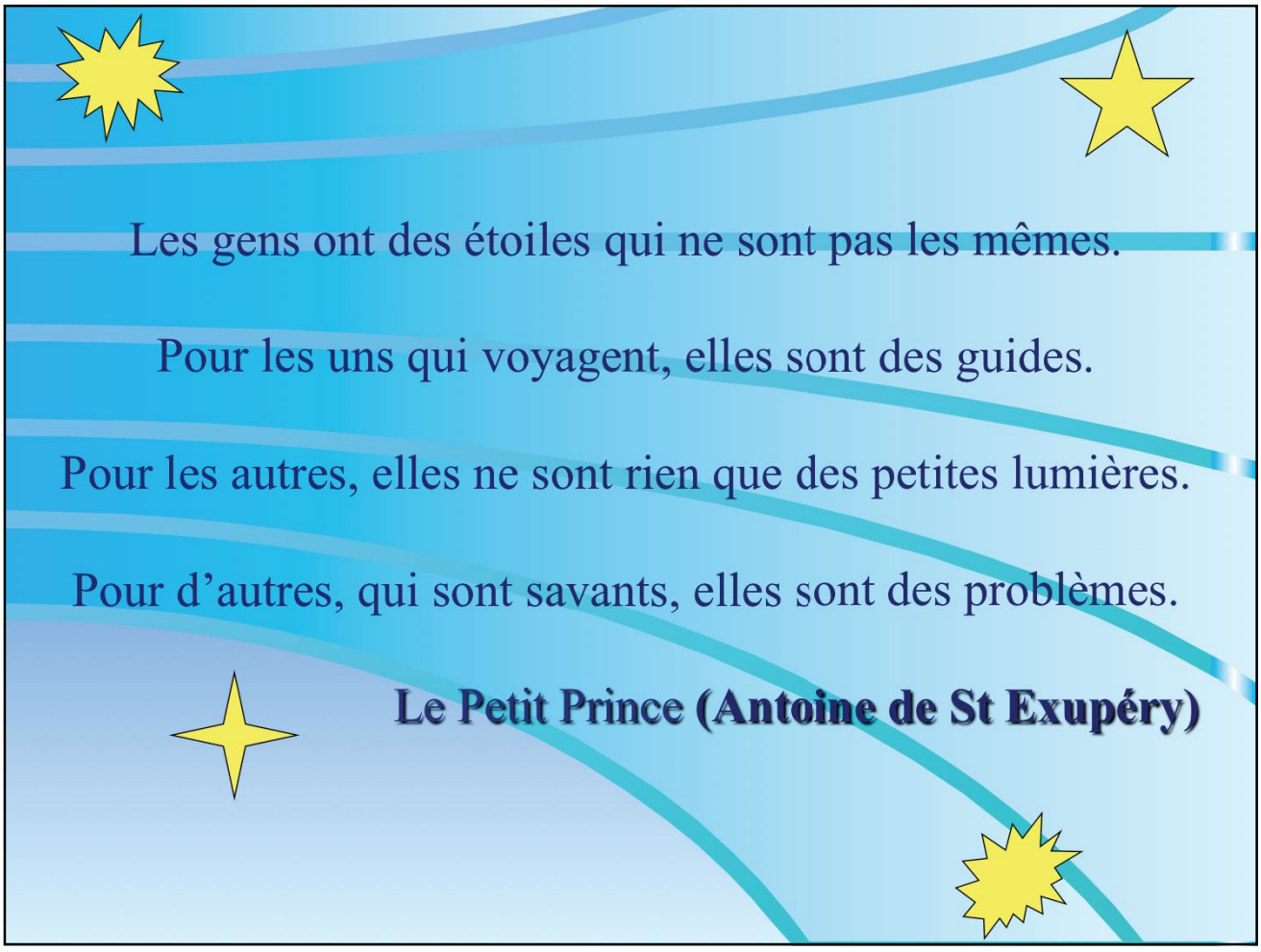
Les gens ont des étoiles qui ne sont pas les mêmes.
Pour les uns qui voyagent, elles sont des guides.
Pour les autres, elles ne sont rien que des petites lumières.
Pour d'autres, qui sont savants, elles sont des problèmes.
Le Petit Prince (Antoine de St Exupéry)

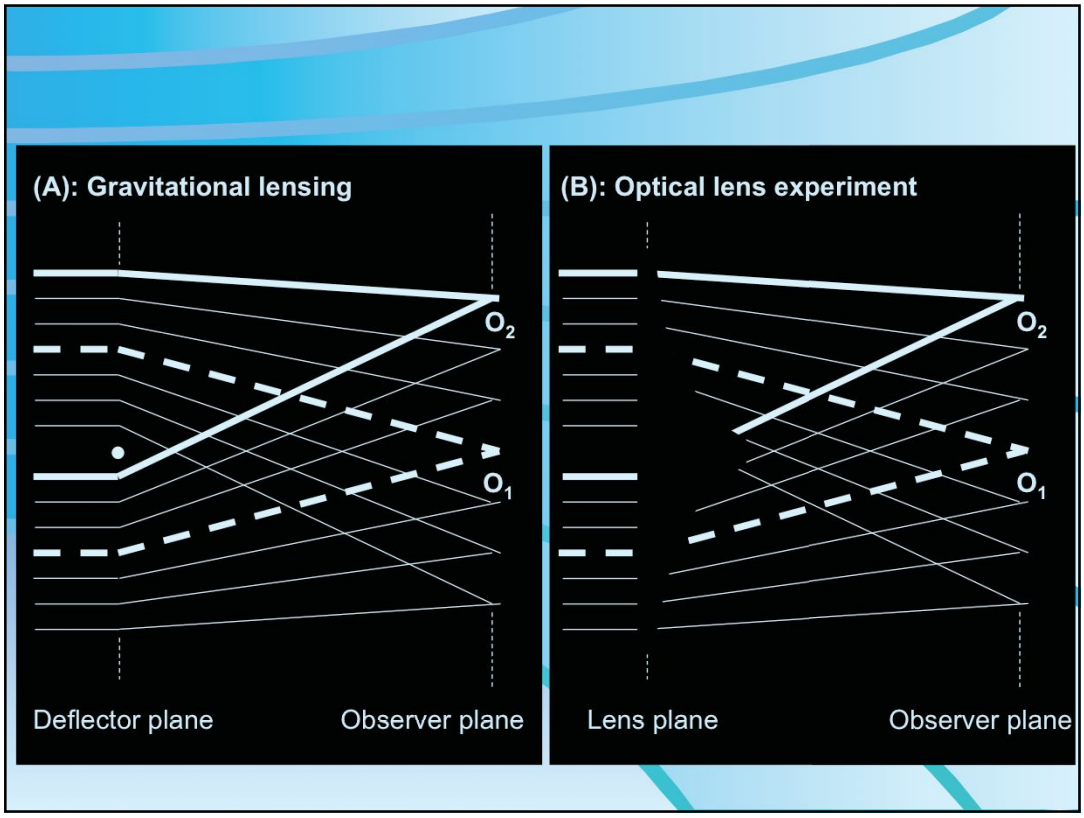
(A): Gravitational lensing
O2
O1
Deflector plane
Observer plane
(B): Optical lens experiment
O2
O1
Lens plane
Observer plane

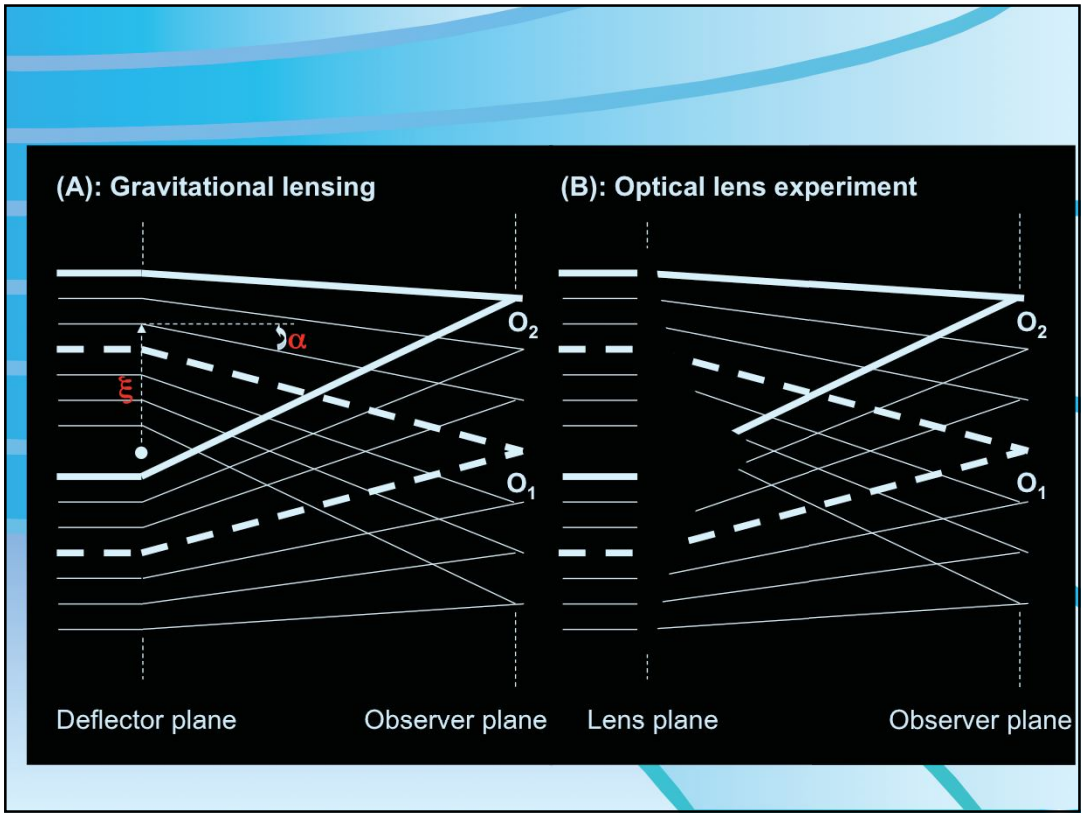
(A): Gravitational lensing
(B): Optical lens experiment
α
ξ1
O2
O1
O2
O1
Deflector plane
Observer plane
Lens plane
Observer plane

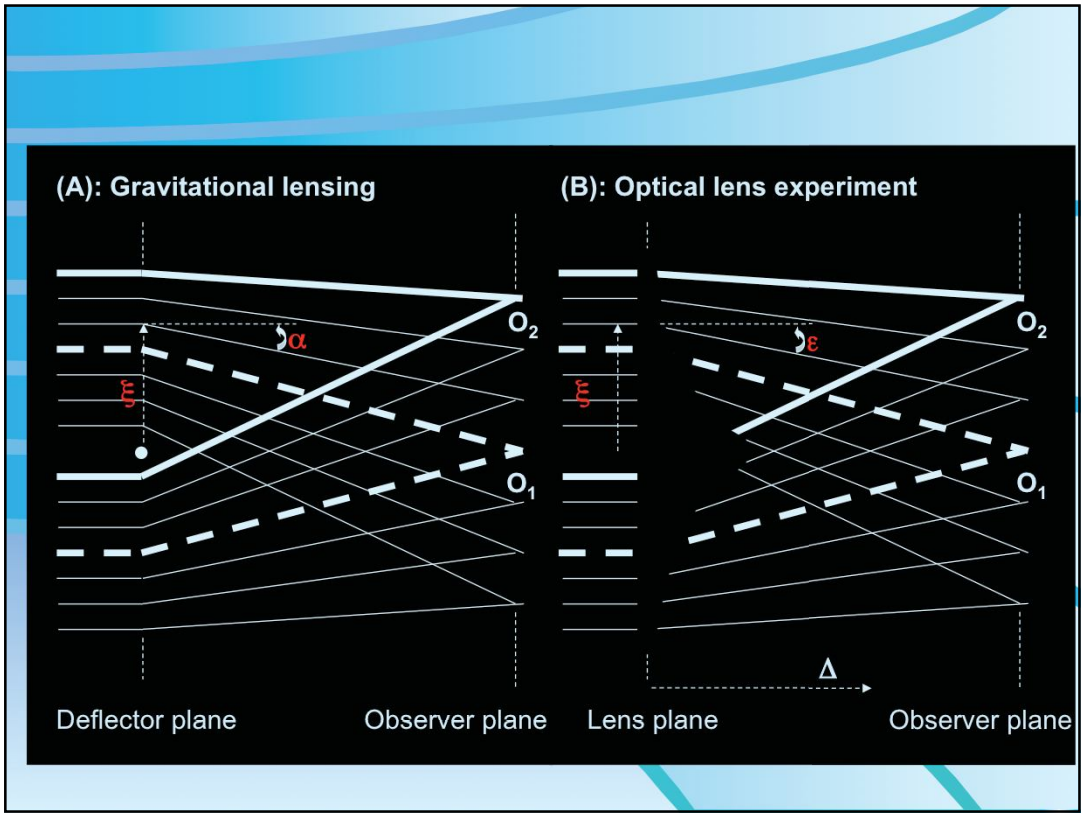
(A): Gravitational lensing
(B): Optical lens experiment
α
ξ
O2
O1
ε
ξ
O2
O1
Δ
Deflector plane
Observer plane
Lens plane
Observer plane

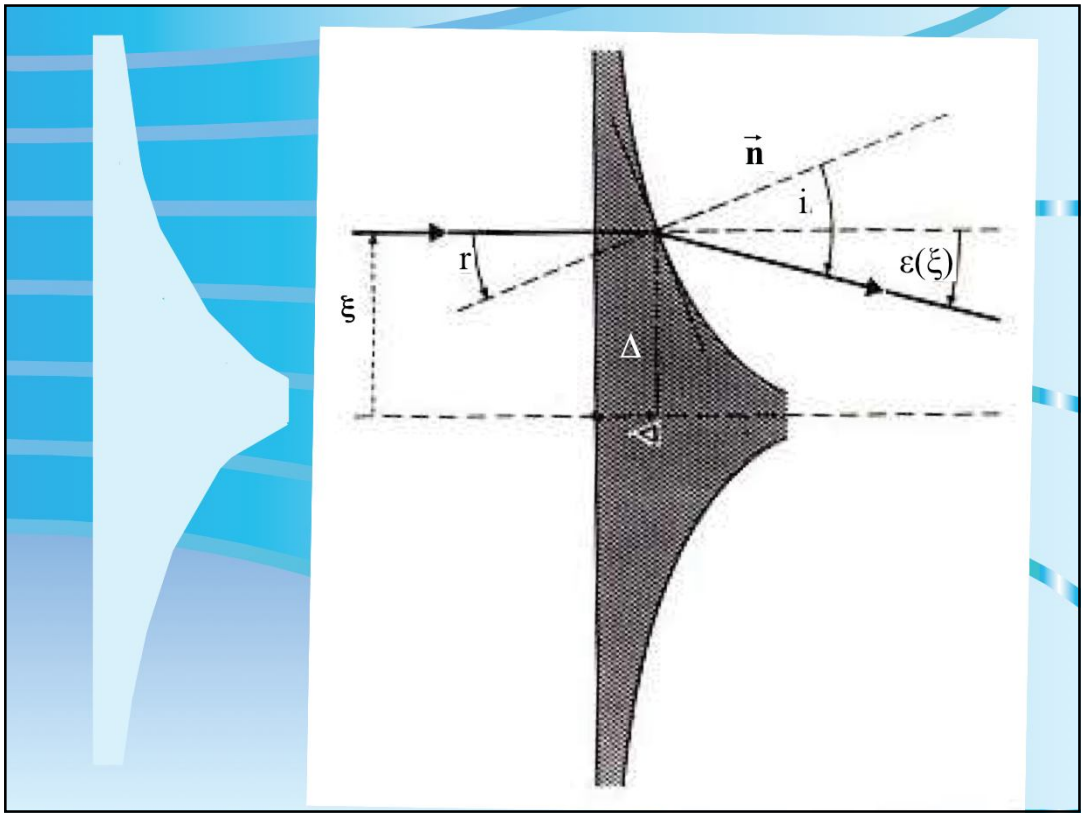
$\vec{n}$
i
r
ε(ξ)
ξ
Δ

2. Gravitational lenses

5. THE OPTICAL GRAVITATIONAL LENS (GL) EXPERIMENT:

5.1. Shapes of axially symmetric optical lenses:

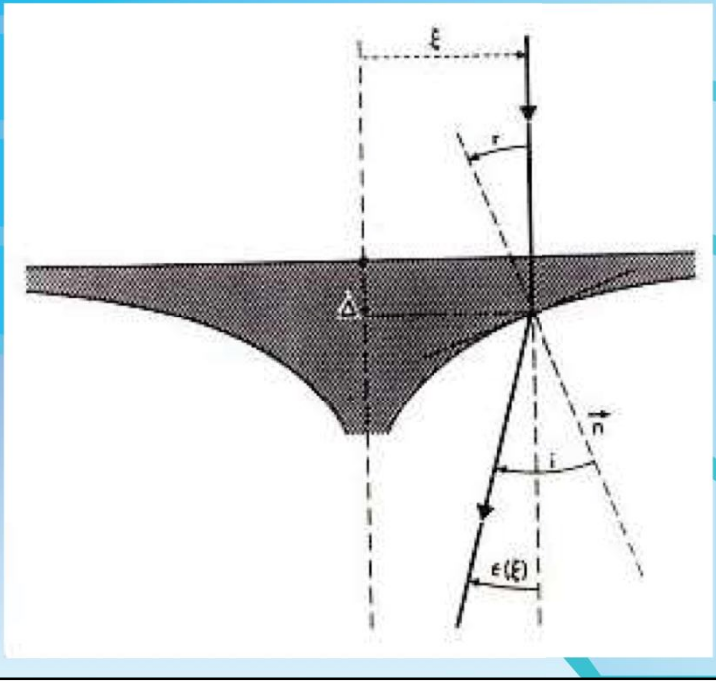

Deflection of a light ray passing through an axially symmetric optical lens.

2. Gravitational Lenses; 5. THE OPTICAL GRAVITATIONAL LENS EXPERIMENT:

For didactical purposes (see the applications in section 6), it is very useful to construct and use optical lenses that mimic the deflection of light rays as derived in Eq.(4.5) for the case of axially symmetric gravitational lenses. Such optical lenses should of course be rotationally symmetric, flat on one side (for simplicity) and have, on the other side, a surface determined in such a way that rays characterized by an impact parameter ξ gets deflected by the angle $\varepsilon(\xi) = \underline{\alpha}(\xi)$ (see Eq.(4.5) and the above figure)

5.1. Shapes of axially symmetric optical lenses:

Applying Descartes's law (cf. Eq.(3.2)) to the ray depicted in the above figure and assuming that the angles (r and i) between the normal **n** to the optical surface and the incident and refracted rays are very small, we may write the relation

$$n = \frac{\sin(i)}{\sin(r)} \approx \frac{i}{r} \qquad (5.1)$$

where n represents here the refractive index of the lens with respect to the air. Furthermore, since we have

$$i = \varepsilon(\xi) + r = \frac{4GM(\xi)}{c^2 \xi} + r \qquad (5.2)$$

and that the tangent to the optical surface at the point (ξ, Δ) is merely given by (see the above figure, Δ stands for the thickness of the lens)

2. Gravitational lenses

5. THE OPTICAL GL EXPERIMENT:

5.1. Shapes of axially symmetric optical lenses:

$$n = \frac{\sin(i)}{\sin(r)} \approx \frac{i}{r}, \qquad (5.1)$$

$$i = \varepsilon(\xi) + r = \frac{4GM(\xi)}{c^2 \xi} + r, \qquad (5.2)$$

$$\frac{d\Delta}{d\xi} = -r, \qquad (5.3)$$

$$\frac{d\Delta}{d\xi} = \frac{-4GM(\xi)}{(n-1)c^2 \xi}, \qquad (5.4)$$

$$\Delta(\xi) = \Delta(\xi_0) + \frac{2R_{sc}}{n-1} \ln\left(\frac{\xi_0}{\xi}\right). \qquad (5.5)$$

2. Gravitational Lenses:

5. THE OPTICAL GRAVITATIONAL LENS EXPERIMENT:

5.1. Shapes of axially symmetric optical lenses:

$$\frac{d\Delta}{d\xi} = -r \qquad (5.3)$$

it is straightforward to derive the shape of a lens by means of the following differential equation

$$\frac{d\Delta}{d\xi} = \frac{-4GM(\xi)}{(n-1)c^2 \xi} \qquad (5.4)$$

5.1.1. The optical point mass lens:

By definition, the mass M of a point lens model is concentrated in one point such that we have M (ξ) = M. It is then simple to solve Eq.(5.4) and derive the thickness Δ(ξ) of the corresponding optical lens as a function of the impact parameter ξ. We find that

$$\Delta(\xi) = \Delta(\xi_0) + \frac{2R_{sc}}{n-1} \ln\left(\frac{\xi_0}{\xi}\right) \qquad (5.5)$$

where R_{sc} represents the Schwarzschild radius of the compact lens (cf. Eq. (4.1)). In practice, the point (ξ_0, $\Delta(\xi_0)$) is chosen in order to specify a given thickness (e.g. $\Delta(\xi_0)$ = 1 cm) for the optical lens at a selected radius (e.g. ξ_0 = 15 cm). The resulting shape of such an optical 'point mass' lens is illustrated on the next figures (see Fig. a on left and the left lens on the right photograph).

2. Gravitational lenses

5. THE OPTICAL GL EXPERIMENT:

5.1. Shapes of axially symmetric optical lenses:

Below: several examples of axially symmetric optical lenses simulating the light deflection properties due to a point mass (a), a SIS galaxy (b), a spiral galaxy (c), a uniform disk (d) and a truncated uniform disk of matter (e).

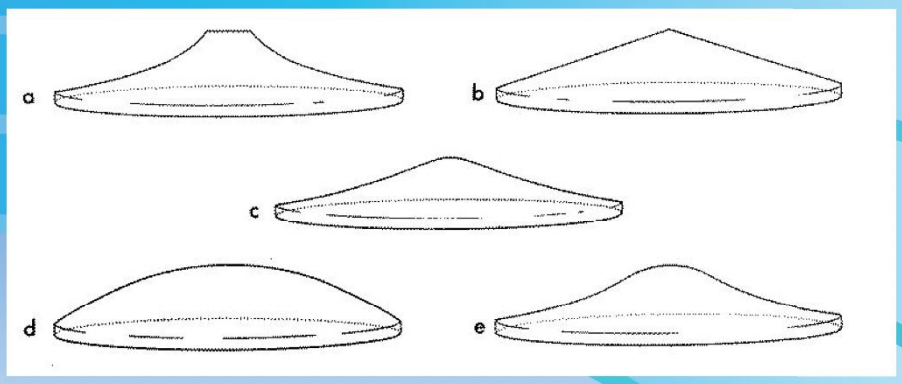

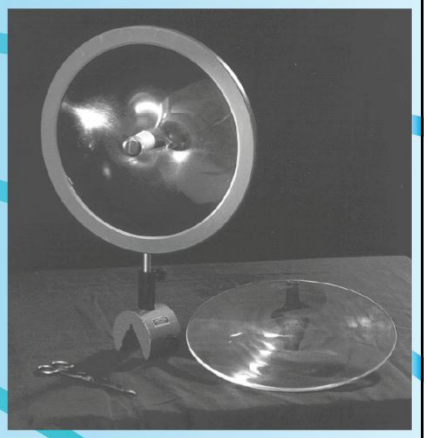

Right: examples of (upper left) a 'point mass' lens (28 cm in diameter) manufactured at the Hamburg Observatory and of (lower right) a 'spiral galaxy' optical lens (30 cm in diameter) produced by the authors at the European Southern Observatory (Garching bei München).

2. Gravitational Lenses:

5. THE OPTICAL GRAVITATIONAL LENS EXPERIMENT:

5.1. Shapes of axially symmetric optical lenses; 5.1.1. The optical point mass lens:

It looks very much like the foot of some glasses of wine which, therefore, have been commonly used in the past by well known astronomers to simulate lensing effects. A realistic 'point mass' lens, made of plexiglas-like material (refractive index n = 1.49 and a diameter of 28 cm), has been manufactured at the Hamburg Observatory for the particular value of R_{sc} = 0.3 cm. This corresponds in fact to the Schwarzschild radius of one third of the Earth mass. We have used such lenses (see the above models on the photograph and the simulations presented during the lectures), made of plexiglas-like material (n = 1.49), to simulate the formation of multiple images of a distant source (see section 6). Our optical gravitational lens experiment is described in section 5.2. Very recently (October 2006), we have begun a mass production of point mass lenses in plexiglas with the following characterization : diameter of 15 cm, n = 1.49 and an equivalent Schwarzschild radius of R_{sc} = 0.6 cm, corresponding to a black hole with a mass of 2/3 that of the Earth.

5.1.2. The SIS optical lens:

For the case of a singular isothermal sphere (hereafter SIS) lens model, it is well known that the mass of such a galaxy increases linearly with the impact parameter ξ, i.e. $M(\xi) \propto \xi$. We may thus rewrite Eq. (5.4) in the form

$$d\Delta / d\xi = -K, \qquad (5.6)$$

where K represents a positive constant. Integration of the above equation leads to the solution

$$\Delta(\xi) = \Delta(\xi_0) + K (\xi_0 - \xi). \qquad (5.7)$$

2. Gravitational lenses

5. THE OPTICAL GL EXPERIMENT:

5.1. Shapes of axially symmetric optical lenses:

$$d\Delta / d\xi = -K, \qquad (5.6)$$

$$\Delta(\xi) = \Delta(\xi_0) + K\,(\xi_0 - \xi). \qquad (5.7)$$

$$\Sigma(\xi) = \Sigma_0 \exp(-\xi / \xi_c) \qquad (5.8)$$

$$M(\xi) = 2\pi \int_0^{\xi} \Sigma(\xi')\,\xi'\,d\xi', \qquad (5.9)$$

$$M(\xi) = 2\pi \xi_c^2 \Sigma_0 \left[1 - \exp(-\xi / \xi_c)\left((\xi / \xi_c) + 1\right)\right], \qquad (5.10)$$

2. Gravitational Lenses:

5. THE OPTICAL GRAVITATIONAL LENS EXPERIMENT:

The shape of the resulting SIS lens is thus merely an axially symmetric cone as illustrated in Fig. b (what would be the shape of such a reflecting lens?).

5.1. Shapes of axially symmetric optical lenses; 5.1.3. The 'spiral galaxy' optical lens:

Given the exponential surface mass density (cf. the similar surface brightness distribution)

$$\Sigma(\xi) = \Sigma_0 \exp(-\xi / \xi_c)\ , \qquad (5.8)$$

which describes reasonably well the mass distribution of a spiral galaxy disk having a characteristic size ξ_c, we may derive the mass distribution $M(\xi)$ of such a deflector by means of the relation

$$M(\xi) = 2\pi \int_0^{\xi} \Sigma(\xi')\,\xi'\,d\xi', \qquad (5.9)$$

Integration of this last expression leads immediately to the result

$$M(\xi) = 2\pi \xi_c^2 \Sigma_0 \left[1 - \exp(-\xi / \xi_c)\left((\xi / \xi_c) + 1\right)\right] \qquad (5.10)$$

Inserting this result into Eq. (5.4) and performing the integration, we find that

$$\Delta(\xi) = \Delta(\xi_0) + \frac{8\pi G \xi_c^2 \Sigma_0}{(n-1)c^2}\left[\ln\left(\frac{\xi_0}{\xi}\right) - \exp\left(\frac{-\xi}{\xi_c}\right) + \exp\left(\frac{-\xi_0}{\xi_c}\right) + \int_{\xi_0/\xi_c}^{\xi/\xi_c} \frac{\exp(-z)}{z}\,dz\right] \qquad (5.11)$$

The general shape of a 'spiral galaxy' optical lens is illustrated in the previous Fig. c. A 30 cm diameter 'spiral galaxy' lens, produced by the authors at the European Southern Observatory

2. Gravitational lenses

5. THE OPTICAL GL EXPERIMENT:

5.1. Shapes of axially symmetric optical lenses:

$$\Delta(\xi) = \Delta(\xi_0) + \frac{8\pi G \xi_c^2 \Sigma_0}{(n-1)c^2}\left[\ln\left(\frac{\xi_0}{\xi}\right) - \exp\left(\frac{-\xi}{\xi_c}\right) + \exp\left(\frac{-\xi_0}{\xi_c}\right) + \int_{\xi_0/\xi_c}^{\xi/\xi_c} \frac{\exp(-z)}{z} dz\right], \quad (5.11)$$

$$M(\xi) = \pi \Sigma_0 \xi^2, \text{ if } \xi \le \xi_c, \quad (5.12a)$$

$$M(\xi) = \pi \Sigma_0 \xi_c^2, \text{ if } \xi > \xi_c. \quad (5.12b)$$

2. Gravitational Lenses; 5. THE OPTICAL GRAVITATIONAL LENS EXPERIMENT:

5.1. Shapes of axially symmetric optical lenses; 5.1.3. The 'spiral galaxy' optical lens:

This manufactured lens is characterized by the following physical parameters: an equivalent Schwarzschild radius of one third of the Earth mass, i.e. $R_{sc} = 2GM(\xi \rightarrow \infty) / c^2 = 4\pi G \xi_c^2 \Sigma_0 / c^2 =$ 0.3 cm (see Eq. (5.10)), $\xi_c = 2.0$ cm, $\xi_0 = 15$ cm and $\Delta(\xi_0) = 0.7$ cm. We should also like to mention that Vanderriest (1985) has manufactured a similar type of lens (~ 20 cm in diameter) directly from a piece of glass, at the Meudon Observatory.

5.1.4. The uniform disk optical lens:

As we shall see in section 6.1.5., a uniform circular disk of matter leads to a perfect convergence of all incoming light rays from a distant source into a single 'focal' point, assuming that the line-of-sight is perpendicular to the disk. We conclude that a classical converging optical lens constitutes the natural counterpart of such a deflector (cf. Fig. d).

5.1.5. The truncated uniform disk optical lens:

For the case of a truncated uniform disk of matter, let us assume that the surface mass density $\Sigma(\xi)$ is constant ($= \Sigma_o$) for values of the impact parameter ξ in the range $[0, \xi_c]$ and that it is zero outside. We then get

$M(\xi) = \pi \Sigma_0 \xi^2$, if $\xi \le \xi_c$, (5.12a)

and

$M(\xi) = \pi \Sigma_0 \xi_c^2$, if $\xi > \xi_c$. (5.12b)

Inserting these results into Eq. (5.4), a simple integration leads to the solution for the thickness $\Delta(\xi)$ of the optical lens as a function of the impact parameter ξ

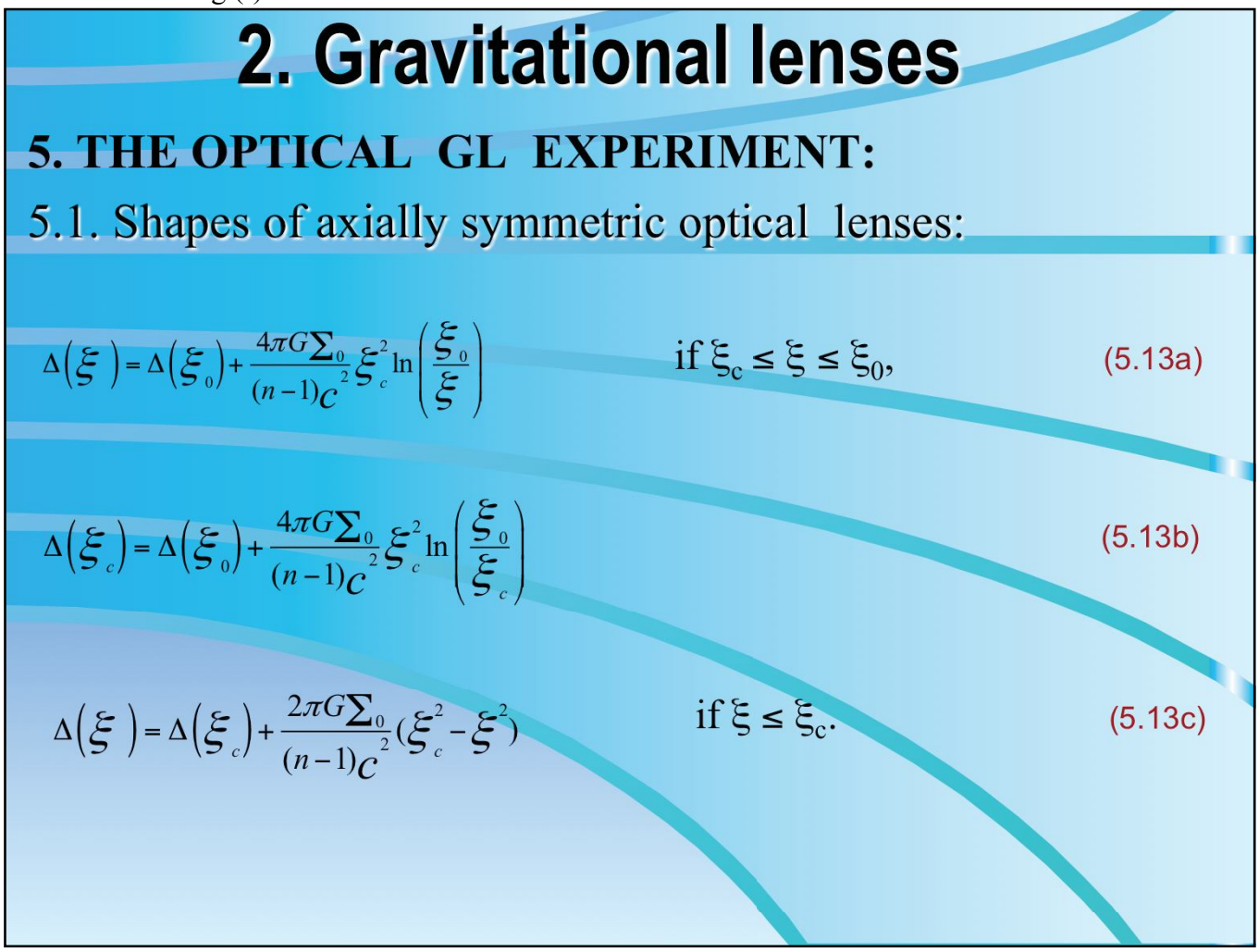

2. Gravitational Lenses:

5. THE OPTICAL GRAVITATIONAL LENS EXPERIMENT:

5.1. Shapes of axially symmetric optical lenses;

5.1.5. The truncated uniform disk optical lens:

$$\Delta(\xi) = \Delta(\xi_0) + \frac{4\pi G\Sigma_0}{(n-1)c^2}\xi_c^2 \ln\left(\frac{\xi_0}{\xi}\right) \quad \text{if} \quad \xi_c \le \xi \le \xi_0 \qquad (5.13a)$$

from which we may derive

$$\Delta(\xi_c) = \Delta(\xi_0) + \frac{4\pi G\Sigma_0}{(n-1)c^2}\xi_c^2 \ln\left(\frac{\xi_0}{\xi_c}\right) \qquad (5.13b)$$

and

$$\Delta(\xi) = \Delta(\xi_c) + \frac{2\pi G\Sigma_0}{(n-1)c^2}(\xi_c^2 - \xi^2) \quad \text{if} \quad \xi \le \xi_c \qquad (5.13c)$$

We have illustrated in a previous figure (see Fig. e) the shape of such an optical lens that simulates the gravitational lensing effects due to a truncated uniform disk of matter.

GL mirage simulator for the case of grazing incidence light reflection (point-like mass lens)

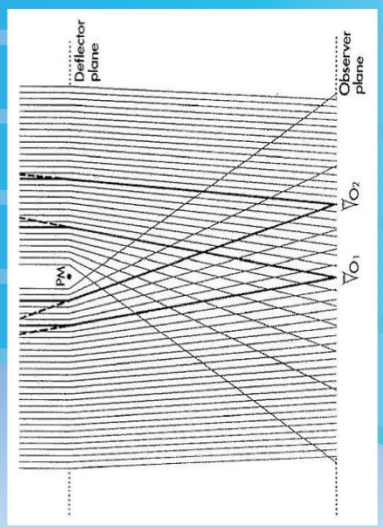

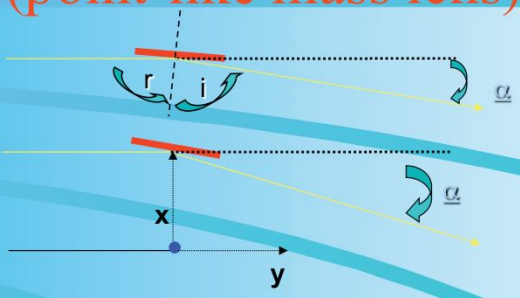

$\alpha = 4GM / (c^2 x)$

$dy/dx = -tg(r)$ with $i + r + \alpha = \pi$, $i = r$, and thus

$r = \pi/2 - \alpha/2$

and finally,

$y = y_0 + K (x_0^2 - x^2)$, with $K = 1/(2 R_{sc})$

GL mirage simulator for the case of grazing incidence light reflection (point-like mass lens)

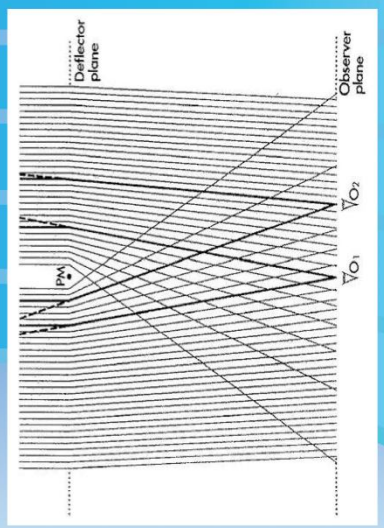

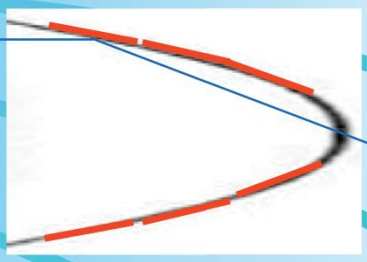

GL mirage simulator for the case of grazing incidence light reflection (point-like mass lens)

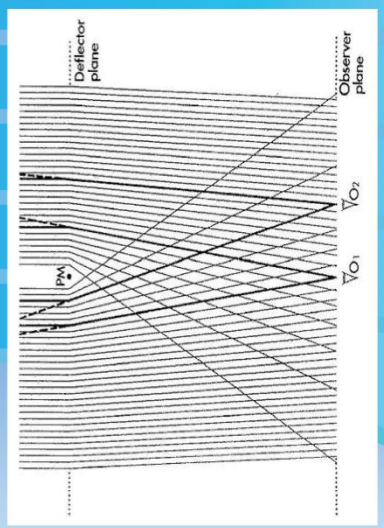

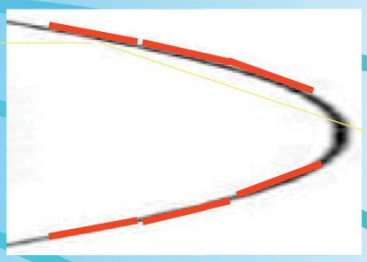

GL mirage simulator for the case of normal incidence light reflection (point- like mass lens)

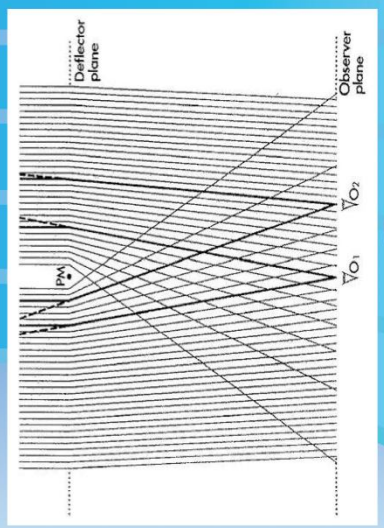

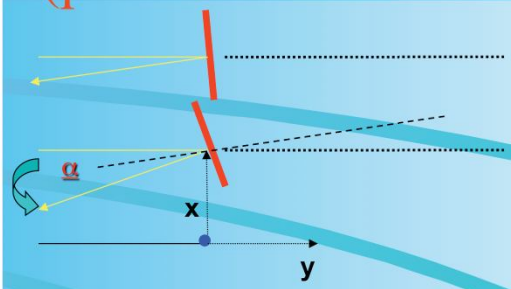

$\underline{\alpha} = 4GM / (c^2 x)$

$dy/dx = -r$ with $i + r = \underline{\alpha}$, $i = r$, and thus

$r = \underline{\alpha}/2$

and finally,

$y = y_0 + K \ln(x_0 / x)$ with $K = Rsc$)

GL mirage simulator for the case of normal incidence light reflection (point- like mass lens)

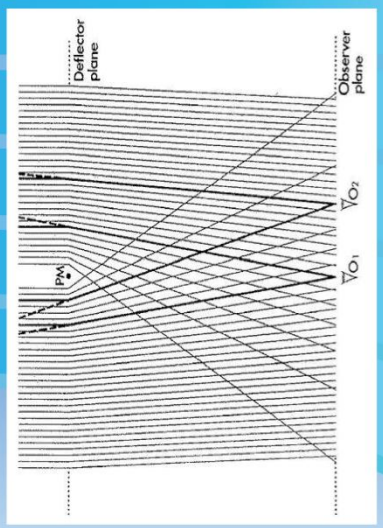

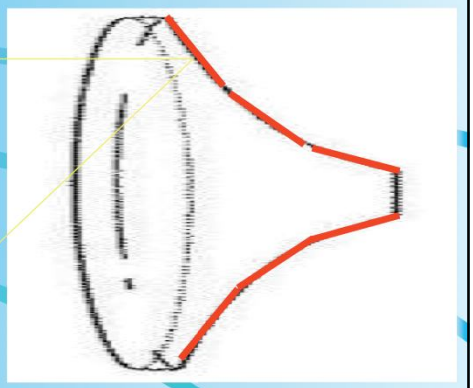

GL mirage simulator for the case of normal incidence light reflection (point- like mass lens)

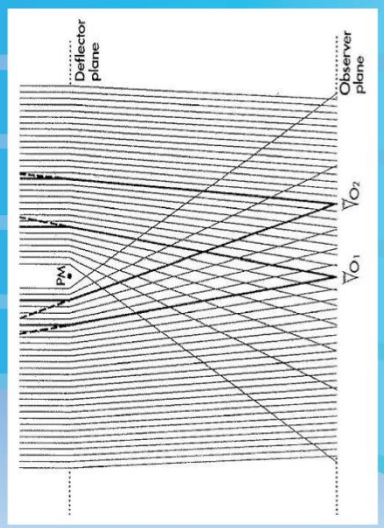

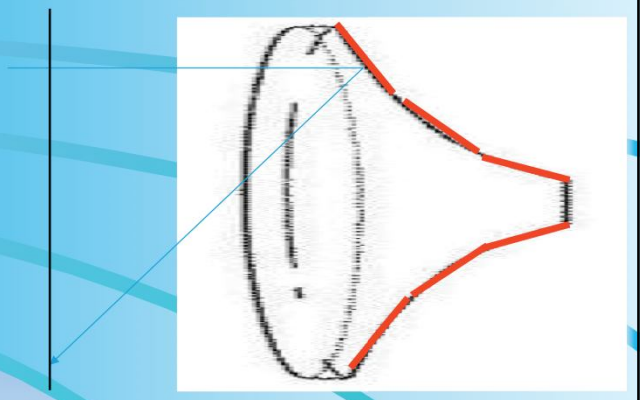

GL mirage simulator for the case of grazing incidence light reflection (uniform disk lens)

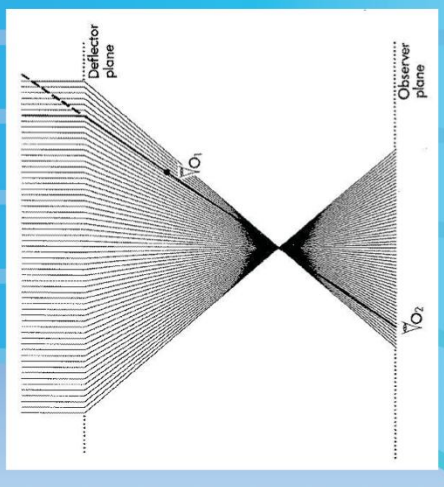

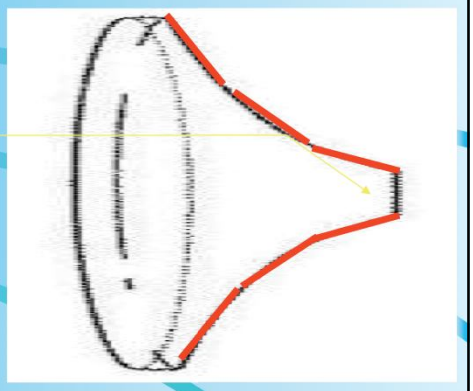

$y = y_0 + K \ln(x_0 / x)$, with $K = c^2/(2G\pi\Sigma_0)$

GL mirage simulator for the case of normal incidence light reflection (uniform disk lens)

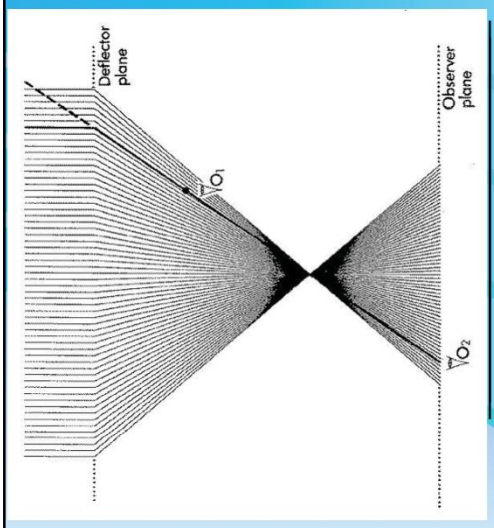

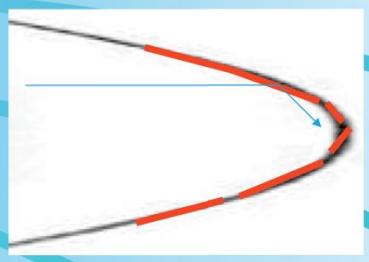

$y = y_0 + K (x_0^2 - x^2)$ with $K = (4G/c^2)\pi\Sigma_0$

The Optical GL Experiment (light relection)

2. Gravitational Lenses:

5. THE OPTICAL GRAVITATIONAL LENS EXPERIMENT: Lens by reflection !

Kamehameha Floral Parade in Waikiki on 10 June 2006 !

2. Gravitational Lenses:

5. THE OPTICAL GRAVITATIONAL LENS EXPERIMENT: Lens by reflection !

Kamehameha Floral Parade in Waikiki on 10 June 2006 !

2. Gravitational Lenses:

5. THE OPTICAL GRAVITATIONAL LENS EXPERIMENT: Lens by reflection !

Kamehameha Floral Parade in Waikiki on 10 June 2006 !

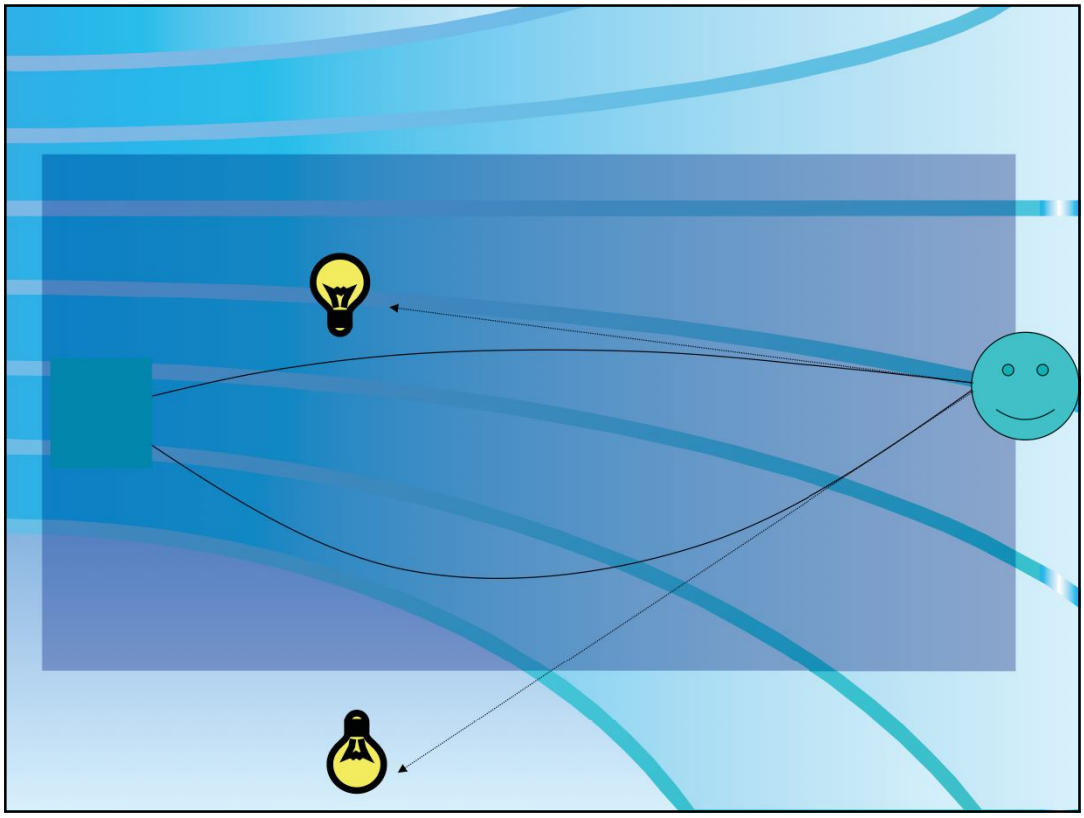


Gravitational lensing inversion

Gravitational lensing inversion

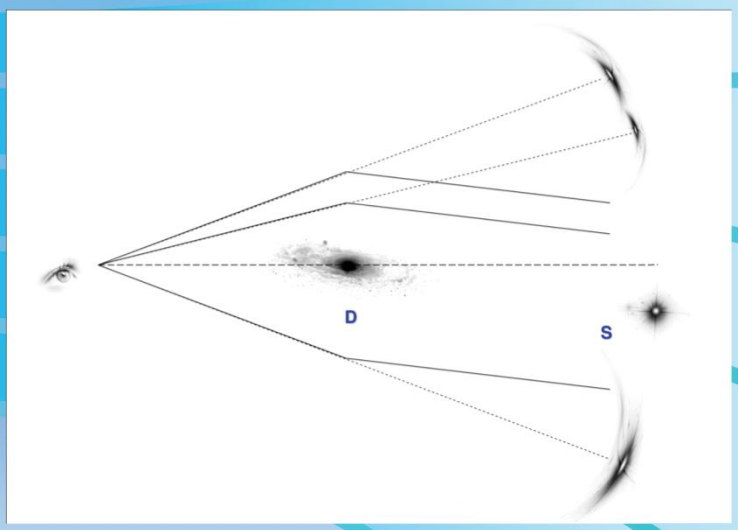

Formation of a 3-lensed image mirage by gravitational lensing.

Gravitational lensing inversion

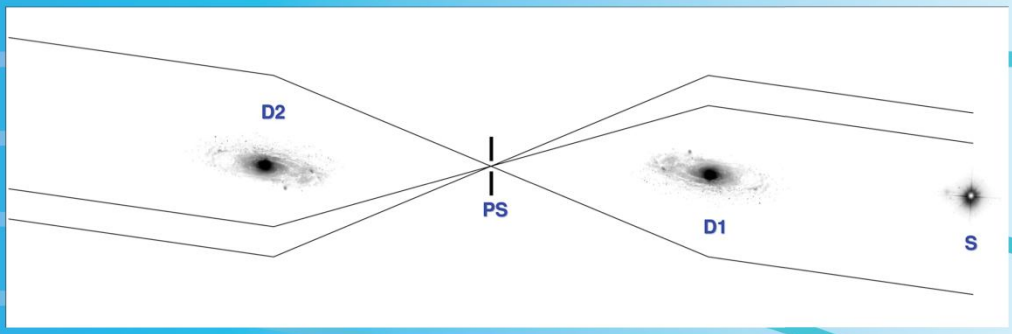

Superposition of the ray tracing diagram shown in the previous figure and a copy of it, rotated by 180°. In this way, we clearly see that the light rays passing through the pinhole screen (PS) get similarly deflected, but in an opposite direction, to those coming from the distant source (S). The three light rays passing the second, inverted, deflecting galaxy (D2) thus continue their travel as a beam of three parallel light rays.

Gravitational lensing inversion

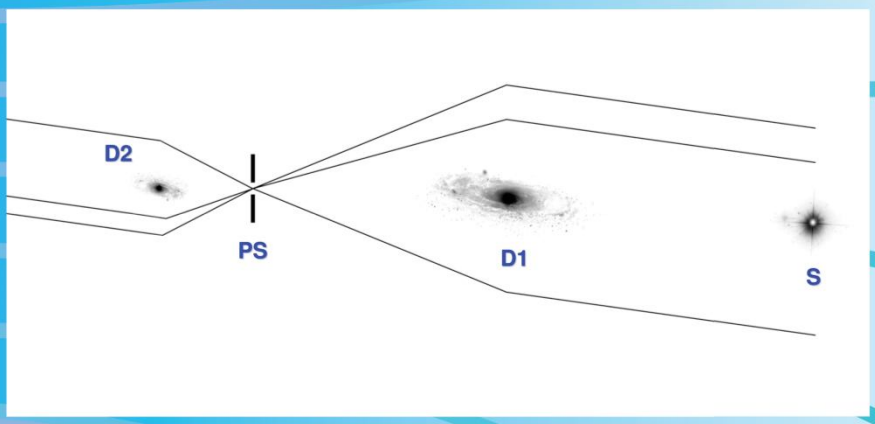

Same as previously but for the case of a deflector (D2) at left being located at a distance three times closer to the pinhole screen (PS) and being also three times less massive than the original deflector (D1)

Gravitational lensing inversion

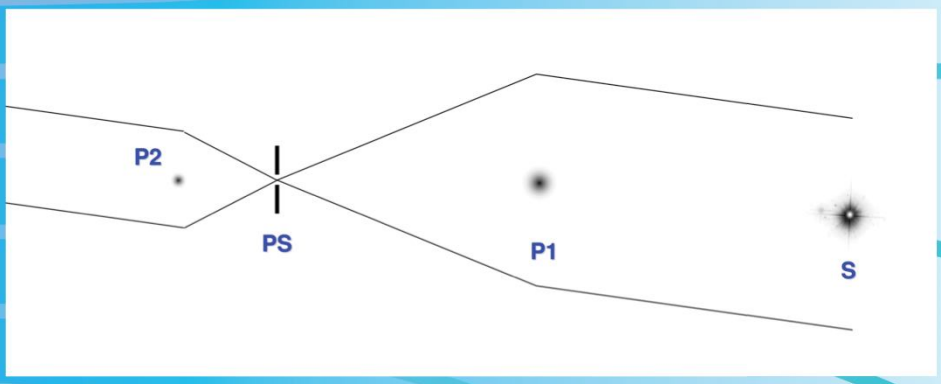

A two lensed image mirage produced by a cosmic point mass lens (P1) at right. The two incoming rays pass through the pinhole screen (PS) and get deflected by a point-mass lens object (P2) at left, at a distance 3 times closer from the pinhole and which mass is also 3 times smaller than that of the original cosmic point mass lens (P1). Alike for the case discussed previously, the outgoing light rays are again parallel.

Gravitational lensing inversion

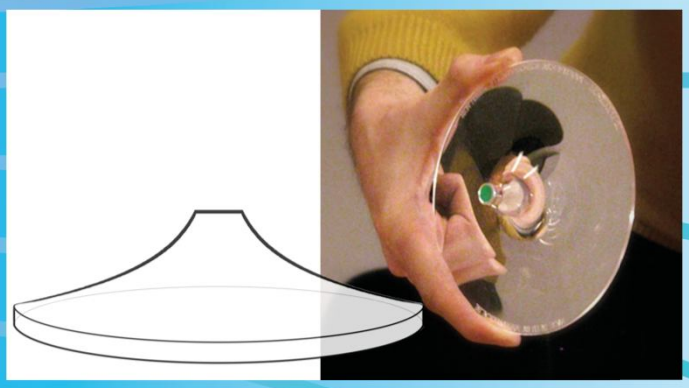

Shape (left) and photograph (right) of an optical lens simulator corresponding to the case of a point mass lens. Such a lens is made of Plexiglas and its shape, similar to the foot of a wine glass, is essentially determined by the mass of the point mass deflector (Refsdal and Surdej 1994).

Gravitational lensing inversion

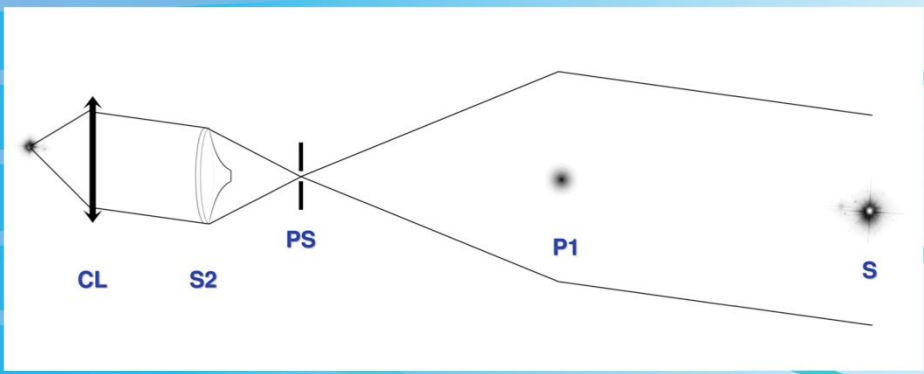

Same as beore but the small size cosmic lens at left (P2) has been replaced by an optical point mass lens simulator (S2) corresponding to the same mass. Since the separation between the two outgoing light rays is now reduced to several tens of centimetres, or even smaller, it is easy to place at left a classical converging lens (CL) so that a perfect, lens inverted image of the distant source at right (S) is formed in its focal plane.

Gravitational lensing inversion

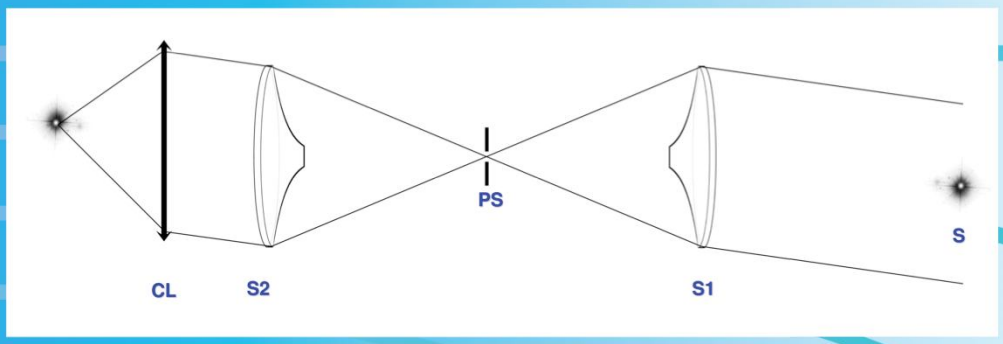

The first point mass gravitational lens simulator (S1) at right produces a doubly imaged source as seen from the pinhole (PS) while the second lens simulator (S2) inverts the mirage into two parallel light rays which are then focused at left by a classical converging lens (CL).

Gravitational lensing inversion

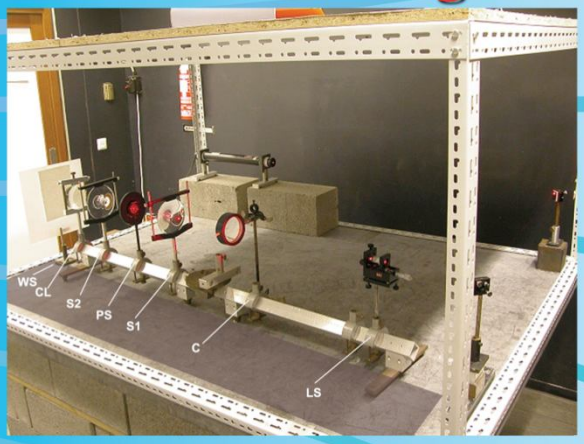

Optical bench in the laboratory showing from right to left the laser point source (LS) obtained with a spatial filter (microscope objective combined with a pinhole screen), followed by a lens (C) that collimates the light rays into a parallel beam which enters the first point mass gravitational lens simulator (S1). Some of the deflected rays then encounter the pinhole screen (PS) and enter the second optical lens simulator (S2). The outgoing light rays are then focused by means of a converging lens (CL) on the white screen (WS) set at the extreme left.

Gravitational lensing inversion

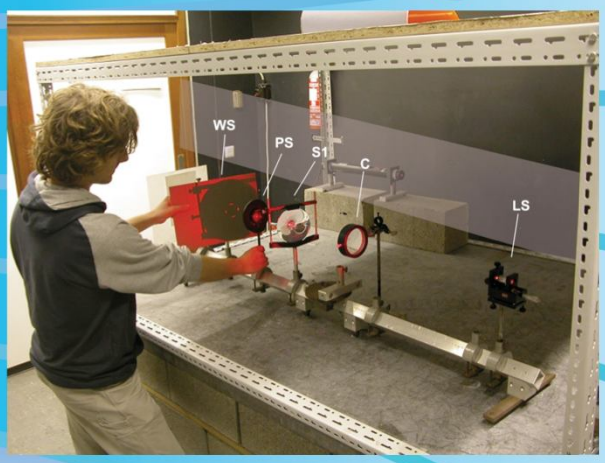

Another view of the laboratory optical bench. In this case, the first point mass gravitational lens simulator (S1) has been somewhat tilted with respect to the optical axis. By placing a white screen (WS) just behind the pinhole screen (PS), one sees the formation of a quadruply imaged source, in accordance with predictions made for the case of a point mass lens in presence of an external shear (see Refsdal and Surdej 1994).

Gravitational lensing inversion

In case of perfect alignment between the source (LS), the pinhole (PS) and the optical lens (S1), set perpendicularly with respect to the axis of the optical bench, there results the formation of an Einstein ring (a) as seen on the white screen (WS) set between the pinhole (PS) and the S2 lens. If we slightly translate along a direction transverse to the optical axis the S1 lens with respect to the pinhole, the Einstein ring breaks in two lensed images (b). If instead, we slightly tilt the S1 lens with respect to the axis of the optical bench, the Einstein ring breaks into four lensed images (c) (see Refsdal and Surdej 1994).

Gravitational lensing inversion

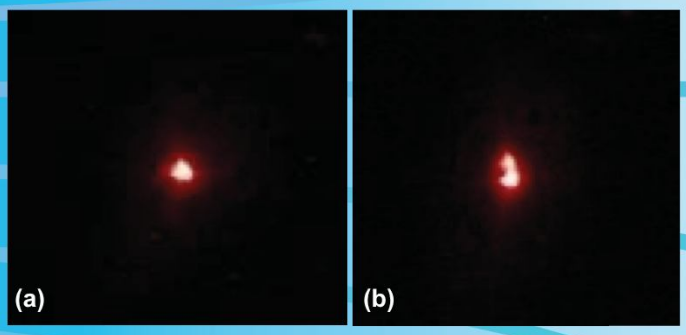

Reconstruction of the inverted lensed images of the laser source on the white screen (WS) placed at the extreme left, for the case of a single (a) point-like source image S and that of a double one (b). The double source was obtained by means of a beam splitter. The diameter of the spot(s) seen in (a) and (b) is approximately 2mm. In these two cases, the S1 and S2 lenses were set perpendicularly to the optical bench axis, slightly translated in opposite transverse directions and symmetrically placed with respect to the pinhole (PS).

Gravitational lensing inversion

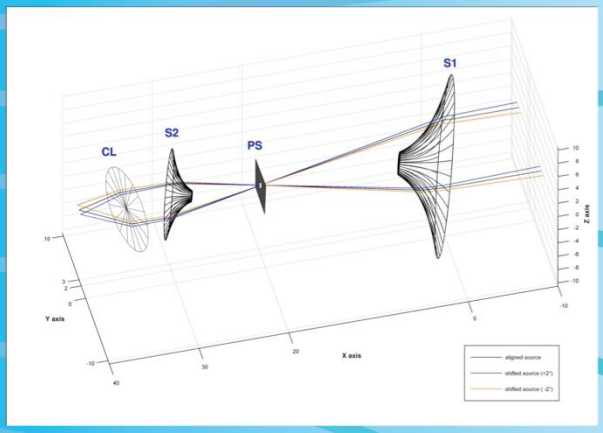

3-D ray tracing simulations performed with the Matlab software for the case of the two optical point mass lens simulators (S1 and S2) being slightly tilted (20°) and translated along the vertical direction with respect to the pinhole (PS). Note that one of the lenses (S2) is twice less massive than the other one (S1) and placed at appropriate distances with respect to the pinhole in order to provide an overall optimal gravitational lens refractor.

Gravitational lensing inversion

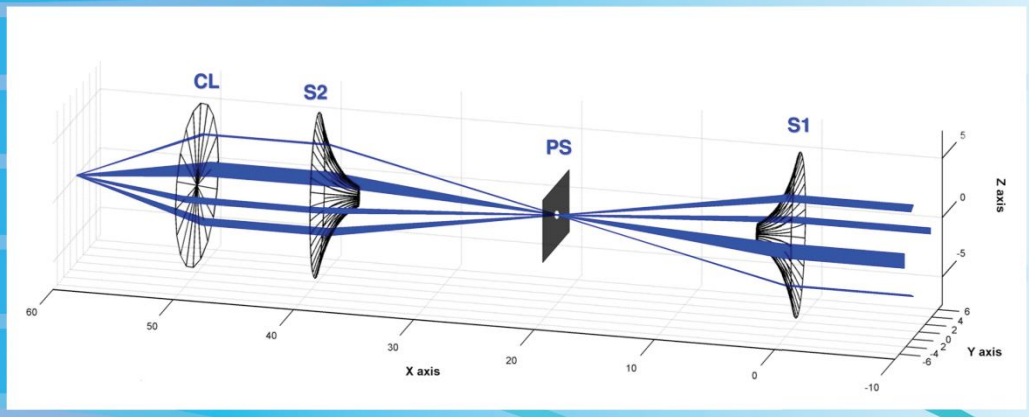

Another example of 3-D ray tracing simulations performed with the Matlab software for the case of the two equal optical point mass lens simulators (S1 and S2) slightly tilted (10°).

Gravitational lensing inversion

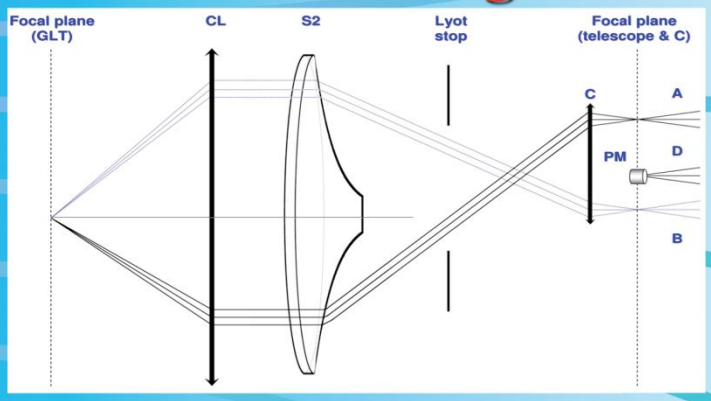

A simple unfolded model of the optimal gravitational lens telescope (OGLT). It is here assumed that the astronomical telescope pointed towards a gravitational lens system produces in its focal plane at right two lensed images (A & B) of a distant point-like source as well as the image of the deflector (D). The latter has been centred on the phase mask (PM) of the coronagraphic device shown in this figure. The lens C collimates the light forming an exit pupil where a Lyot stop is placed. The optical point mass lens simulator S2 then inverts the observed gravitational lens mirage into two parallel beams of light rays which are then focused at left by a classical converging lens (CL). A single image of the original point-like source, observed as a multiply imaged object, has thus been restored in the focal plane of CL.

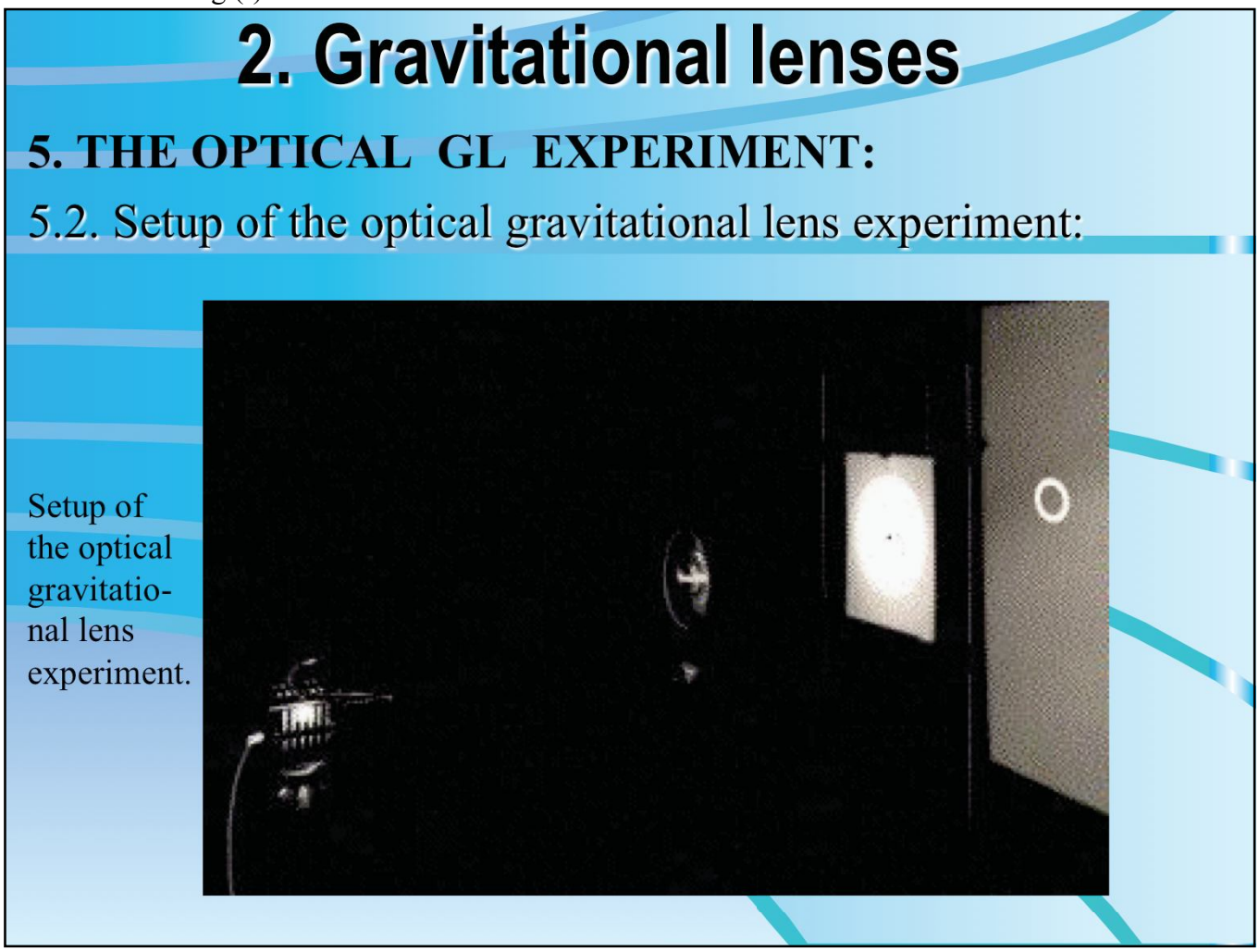

2. Gravitational Lenses:

5. THE OPTICAL GRAVITATIONAL LENS EXPERIMENT:

5.2. Setup of the optical gravitational lens experiment:

In order to simulate the formation of lensed images by a given mass distribution (point mass, etc.), we have used the optical setup that is shown on the next figure.

The optical gravitational lens experiment is composed of a light source (on the left on the picture), the optical lens followed by a white screen with a small hole at the center (pinhole) and further behind, a large screen on which is (are) projected the lensed image(s) of the source as it would be seen if our eye was located at the position of the pinhole (the pinhole corresponds to the observer's eye). In the example illustrated here, the pinhole is set very precisely on the optical axis of the gravitational lens so that the source, the lens and the pinhole (observer) are perfectly aligned. In the present case, the resultant image seen on the screen is an Einstein ring.

Considering other relative positions between the source, the lens and the observer, and also for the additional case of an asymmetric lens, we shall illustrate in section 6 the resulting lensed images as a function of the pinhole position in the observer plane. Note that the bright regions seen on the lens in the figure shown above are caused by scattered light.

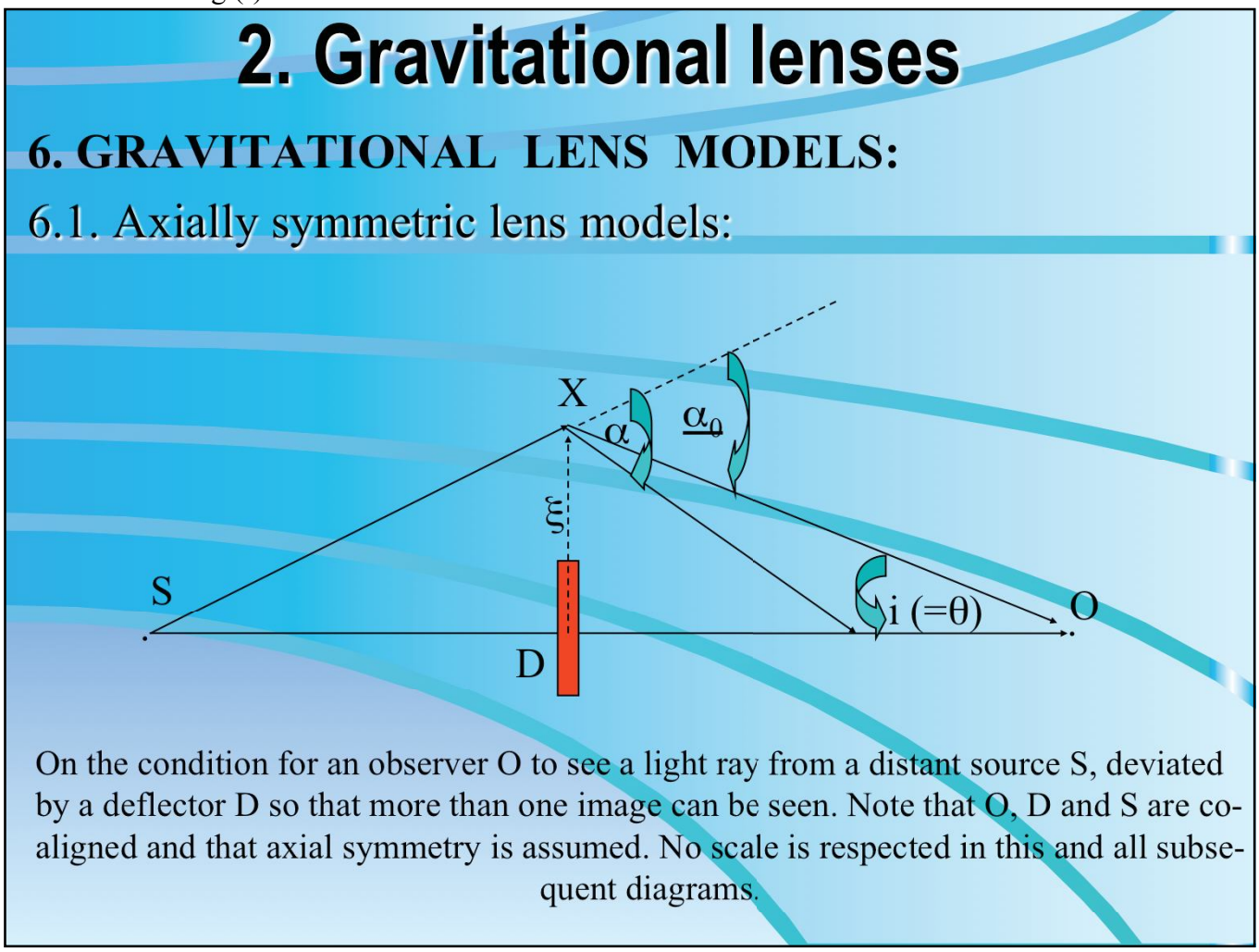

2. Gravitational Lenses:

6. GRAVITATIONAL LENS MODELS:

6.1. Axially symmetric lens models; 6.1.1. Generalities:

In the case of perfect alignment between a source (S), an axially symmetric deflector (D) and an observer (O) (see the above figure), we easily see that, with the exception of the direct ray propagating from the source to the observer, the condition for any other light ray to reach the observer is

$\theta / D_{ds} \sim \underline{\alpha_0} / D_{os}$, (6.1)

as obtained from the direct application of the sine rule to the triangle SXO and assuming that the angles θ and $\underline{\alpha_0}$ remain very small. Of course, this will also be true if the following condition (*) is fulfilled: $\alpha \geq \underline{\alpha_0}$ since it will then be always possible to find a light ray with a larger impact parameter ξ such that Eq. (6.1) is fulfilled. Expressing the angle θ between the direct ray and the incoming deflected ray as

$\theta \sim \xi / D_{od}$, (6.2) and

making use of Eqs. (4.5) and (6.1), we may thus rewrite condition (*) as follows

$\Sigma(\xi' < \xi) \geq \Sigma_c$, (6.3) i.e. the

average surface mass density of the lens

$\Sigma(\xi' < \xi) = M(\xi) / (\pi \xi^2)$, (6.4)

evaluated within the impact parameter ξ, must simply exceed the critical surface mass density Σ_c, defined by

$$\Sigma_c = \frac{c^2}{4\pi G D}, \quad (6.5)$$

2. Gravitational lenses

6. GRAVITATIONAL LENS MODELS:

6.1. Axially symmetric lens models:

$$\theta / D_{ds} \sim \underline{\alpha_0} / D_{os}, \qquad (6.1)$$

$$\theta \sim \xi / D_{od}, \qquad (6.2)$$

$$\Sigma(\xi'<\xi) \geq \Sigma_c, \qquad (6.3)$$

$$\Sigma(\xi'<\xi) = M(\xi) / (\pi\xi^2), \qquad (6.4)$$

$$\Sigma_c = \frac{c^2}{4\pi G D}, \qquad (6.5)$$

$$D = D_{od}\, D_{ds} / D_{os}, \qquad (6.6)$$

2. Gravitational Lenses:

6. GRAVITATIONAL LENS MODELS:

6.1. Axially symmetric lens models; 6.1.1. Generalities:

where $D = D_{od}\, D_{ds} / D_{os}$. (6.6)

Let us note that the latter quantity is essentially determined by the distances between the source, the deflector and the observer. As we shall see in section 6.1.5., a circular disk with uniform surface mass density Σ_c, acts as a perfect converging lens, and we have $\Sigma = \Sigma_c$ for the particular case when the observer is precisely located at its focal point. Although the above reasoning essentially applies to a static Euclidian space, Refsdal (1966b) has shown that it also remains valid for Friedmann, Lemaître, Robertson, Walker (FLRW) expanding universe models, provided that D_{os}, D_{od} and D_{ds} represent angular size distances. Adopting typical cosmological distances for the deflector (redshift $z_d \sim 0.5$) and the source ($z_s \sim 2$), we find that $\Sigma_c \sim 1$ g cm^{-2}.

Substituting $M(\xi)$ and ξ in Eq. (6.4) with a typical mass M and a radius R for the deflector, we have listed in the appended Table values for the ratio $\Sigma(<R) / \Sigma_c$ considering a star, a galaxy and a cluster of galaxies located at various distances. We see that only stars and very compact, massive galaxies and galaxy clusters, for which $\Sigma(<R) / \Sigma_c \geq 1$, constitute promising 'multiple imaging' deflectors.

More precisely, we may write

$$D = \frac{c}{H_0} L(z_d) \left(1 - \frac{\Delta(z_d)}{\Delta(z_s)}\right) \qquad (6.7)$$

2. Gravitational lenses

6. GRAVITATIONAL LENS MODELS:

6.1. Axially symmetric lens models:

$$D = \frac{c}{H_0} L(z_d)\left(1 - \frac{\Delta(z_d)}{\Delta(z_s)}\right) \qquad (6.7)$$

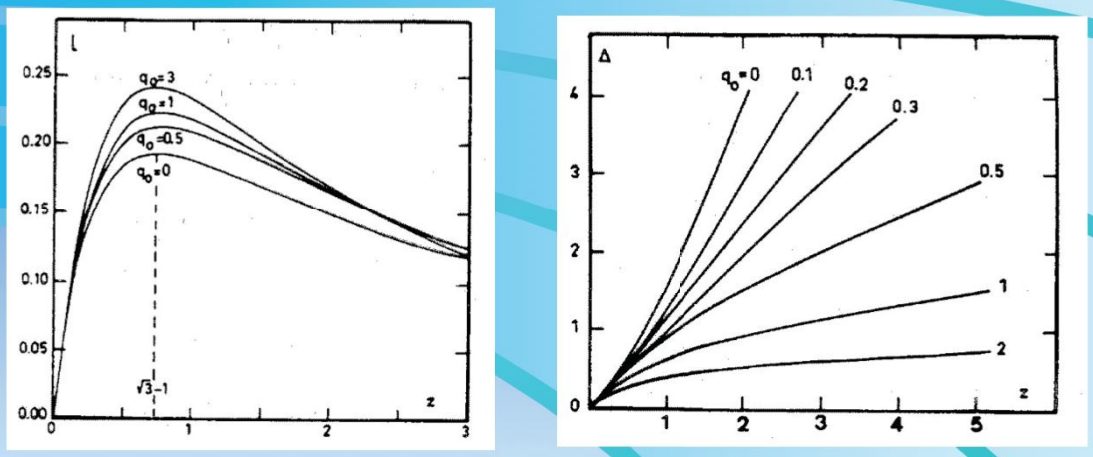

The quantities L(z) and Δ(z) as a function of the redshift z for various cosmological models

2. Gravitational Lenses:

6. GRAVITATIONAL LENS MODELS:

6.1. Axially symmetric lens models, 6.1.1. Generalities:

where $L(z_d)$ is a function presenting a well defined extremum around $z_d \sim 0.7$, almost independently of the adopted cosmological model (see the next figures). A natural conclusion is that foreground objects located near $z_d \sim 0.7$ should prove to be very efficient lenses.

In the case of axial symmetry, it is clear that in the presence of an efficient deflector, an observer located on the symmetry axis will actually see a ring (the so-called 'Einstein ring', cf. the previous photograph) of light from a distant source. Combining Eqs. (4.5)-(6.1) and (6.2), the angular radius of this ring may be conveniently expressed as

$$\theta_E = \sqrt{\frac{4GM\left(R' \le D_{od}\theta_E\right) D_{ds}}{c^2 D_{od} D_{os}}} \qquad (6.8)$$

2. Gravitational lenses

6. GRAVITATIONAL LENS MODELS:

6.1. Axially symmetric lens models:

$$\theta_E = \sqrt{\frac{4GM\left(R' \le D_{od}\theta_E\right)D_{ds}}{c^2 D_{od} D_{os}}} \qquad (6.8)$$

Table: Ratio of the average $\Sigma(R'< R)$ and critical Σ_c surface mass densities, angular (θ_E) and linear (ξ_E) radii of the Einstein ring for different values of the mass M, distance D_{od} and radius R of the deflector, assuming that $D_{os} = 2\ D_{od}$ (1parsec = 1 pc = 3.262 lightyears = $3.086\ 10^{18}$ cm)

Deflector	M	D_{od}	R	$\Sigma(R'<R)/\Sigma_c$	θ_E	$\xi_E = \theta_E\ D_{od}$(pc)
Star	$1\ M_\odot$	10^4 pc	$2\ 10^{-8}$ pc	$2\ 10^6$	$6\ 10^{-4}$"	$3\ 10^{-5}$ pc
Star	$1\ M_\odot$	10^9 pc	$2\ 10^{-8}$ pc	$2\ 10^{11}$	$2\ 10^{-6}$"	10^{-2} pc
Galaxy core	$10^{12}\ M_\odot$	10^9 pc	$5\ 10^3$ pc	4	2"	10^4 pc
Cluster core	$10^{14}\ M_\odot$	10^9 pc	10^5 pc	1	20"	10^5 pc

2. Gravitational Lenses:

6. GRAVITATIONAL LENS MODELS:

6.1. Axially symmetric lens models:

6.1.1. Generalities:

We have also listed in the previous Table typical values of θ_E for different types of deflectors located at various distances. As we shall see in the next sections, the value of θ_E derived above is very important because it can usually be used to estimate the angular separation between multiply imaged sources in more general cases where the condition of a perfect alignment between the source, deflector and observer is not fulfilled or even for lens mass distributions which significantly depart from the axial symmetry. Observed image separations (~ $2\ \theta_E$) can therefore lead to the value of M / D_{od}, or to the value of $M\ H_0$, if the redshifts z_d and z_s are known. This is the simplest and most direct astrophysical application of gravitational lensing. We see from the previous Table that for a source and a lens located at cosmological distances (z_d ~ 0.5 and z_s ~ 2), the angle θ_E can vary from micro-arcsec (stellar deflection) to arcsec (galaxy lensing), and up to some tens of arcsec in the case of cluster lenses. Let us also finally note that the condition (6.3) for a deflector to produce multiple images of a lensed source turns out to be usually applicable, even when there is no axial symmetry. We shall now describe in more detail some of the best known lens models.

2. Gravitational lenses

6. GRAVITATIONAL LENS MODELS:

6.1. Axially symmetric lens models:

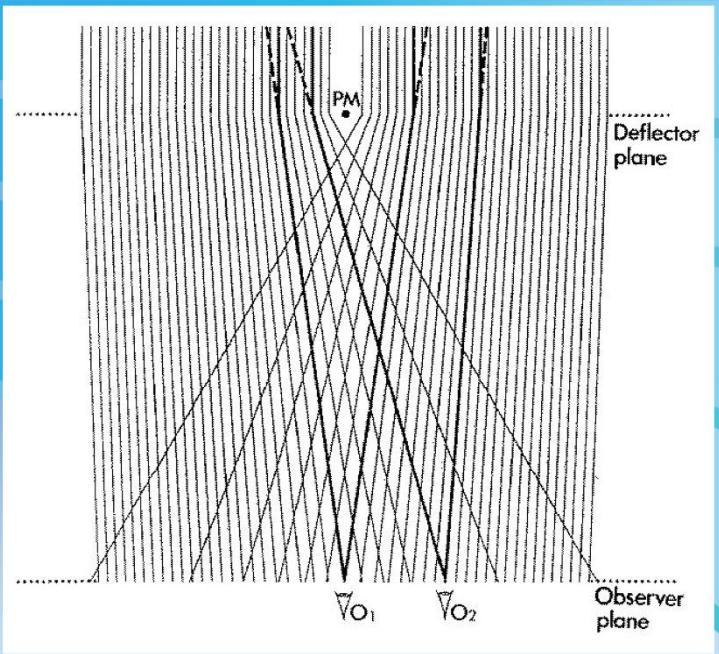

Ray tracing diagram for the point mass (PM) lens model. This diagram, as well as all subsequent ray tracing diagrams represent a set of parallel light rays, originating from a very distant point source, that are deviated as they cross the deflector plane. Different observer positions are represented in the 'observer' plane from where multiple lensed images may usually be seen.

$$\alpha = \frac{2 R_{sc} D_{ds}}{\theta D_{od} D_{os}} = \theta - \theta_s \qquad (6.7)$$

2. Gravitational Lenses:

6. GRAVITATIONAL LENS MODELS:

6.1. Axially symmetric lens models:

6.1.2. The point-mass lens model:

We first consider the classical model consisting of a single point mass (cf. a black hole or a very compact object). Due to the axial symmetry, the propagation of light rays essentially reduces to a one dimensional problem. Given the deflection angle in Eq. (4.1), the lens equation (4.3) may thus be rewritten as

$$\alpha = \frac{2 R_{sc} D_{ds}}{\theta D_{od} D_{os}} = \theta - \theta_s \qquad (6.7)$$

We have used this result to illustrate in the upper figure a typical ray tracing diagram for the model of a point mass lens. In the case of perfect alignment between the source, the lens and the observer, the latter (see O_1 in the above figure and see inset (a) on the next set of photographs) sees a ring of light due to the symmetry (cf. the Einstein ring in the gravitational lens experiment previously shown). As the observer moves away from the symmetry axis (cf. O_2 in the above figure and insets (b) and (c) on next page), the Einstein ring breaks up in two images that are located in the direction of the deflected rays, on opposite sides of the deflector.

2. Gravitational lenses

6. GRAVITATIONAL LENS MODELS:

6.1. Axially symmetric lens models:

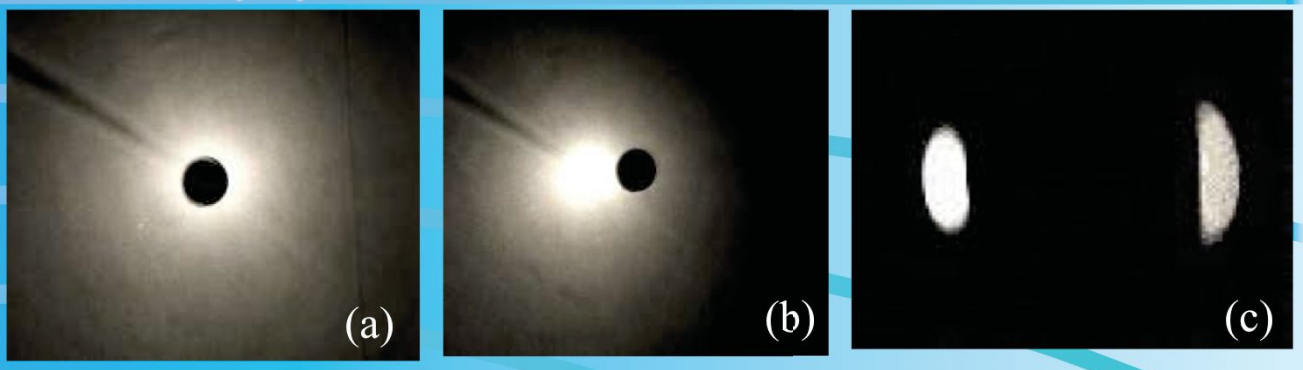

Optical gravitational lens experiment: in this first experiment used to simulate the gravitational deflection of light rays by a point mass lens model (see section 5.2.), the pinhole (observer) is set very precisely on the optical axis of the gravitational lens so that the source, the lens and the observer are perfectly aligned (a). The resulting image is an Einstein ring (see the ring on a previous photograph). As the pinhole is moved slightly away from the symmetry axis (b), the Einstein ring breaks up in two images (c).

2. Gravitational Lenses:

6. GRAVITATIONAL LENS MODELS:

6.1. Axially symmetric lens models:

6.1.2. The point-mass lens model:

The solutions of the lens equation may be obtained in a simple way from a bending angle diagram (see next figure) where the quantities $\alpha(\theta)$ and $\theta - \theta_s$ are plotted as a function of θ and where the intersections between the hyperbola (i.e. $\alpha(\theta)$) and the straight line (i.e. $\theta - \theta_s$) passing through the point (θ_s, 0) correspond to the desired solutions. For a given circular source S, it is then straightforward to construct geometrically the resulting images projected on the sky, as seen by an observer for the two cases of perfect and non perfect alignments (cf. the insets (a) and (c) in the next figure, respectively).

2. Gravitational lenses

6. GL MODELS:

6.1. Axially symmetric lens models:

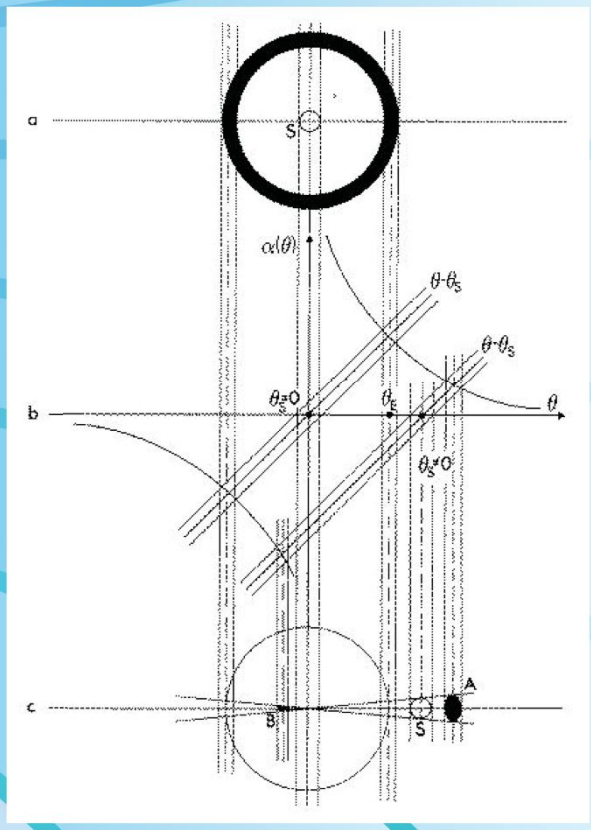

Combined bending angle diagram (b) and resulting lensed images (a and c) produced for the circular source S by a point mass lens model. In this and all subsequent bending angle diagrams, the solutions (θ) of the lens equation (see Eq. (4.3)) are obtained from the geometric intersections between the bending curve α(θ) and the straight line θ- θ_s, for the case of a circular source S whose center is located at a true angular distance θ_s from the deflector. The resulting lensed images are then constructed from simple geometric projections, using compasses. For the particular case $\theta_s = 0$, the circular source S is lensed into an Einstein ring whose angular radius is θ_E (a).

2. Gravitational Lenses; 6. GRAVITATIONAL LENS MODELS:

6.1. Axially symmetric lens models; 6.1.2. The point-mass lens model:

Finally, an alternative way to solve the lens equation (6.7) is to make use of the results (4.1) and (6.6) and to rewrite the former equation as follows

$$\theta^2 - \theta_s \theta - \theta_E^2 = 0 \qquad (6.8)$$

so that the two solutions may be simply expressed as

$$\theta_{A,B} = \frac{\theta_s}{2} \pm \sqrt{\left(\frac{\theta_s}{2}\right)^2 + \theta_E^2} \qquad (6.9)$$

For $\theta_s = 0$, we find of course that the angular radius of the Einstein ring is given by $\theta_{A,B} = \pm \theta_E$ and by means of Eq. (4.6) that the magnification of this ring is

$$\mu_E = 2\theta_E / d\theta_s \qquad (6.10)$$

where $d\theta_s$ ($<< \theta_E$) represents the true angular radius of the source. As we depart from perfect alignment (i.e. $\theta_s \neq 0$), it is easy to show (see Eqs. (6.9) and (4.6)) that the angular separation between the two inverted, lensed, images is

$$\Delta\theta = \theta_A - \theta_B = \sqrt{\theta_s^2 + 4\theta_E^2} \qquad (6.11)$$

and that their positive (A is a direct image) and negative (B is inverted) magnification is

$$\mu_{A,B} = \frac{1}{4}\left(2 \pm \left(\frac{\Delta\theta}{\theta_s} + \frac{\theta_s}{\Delta\theta}\right)\right) \qquad (6.12)$$

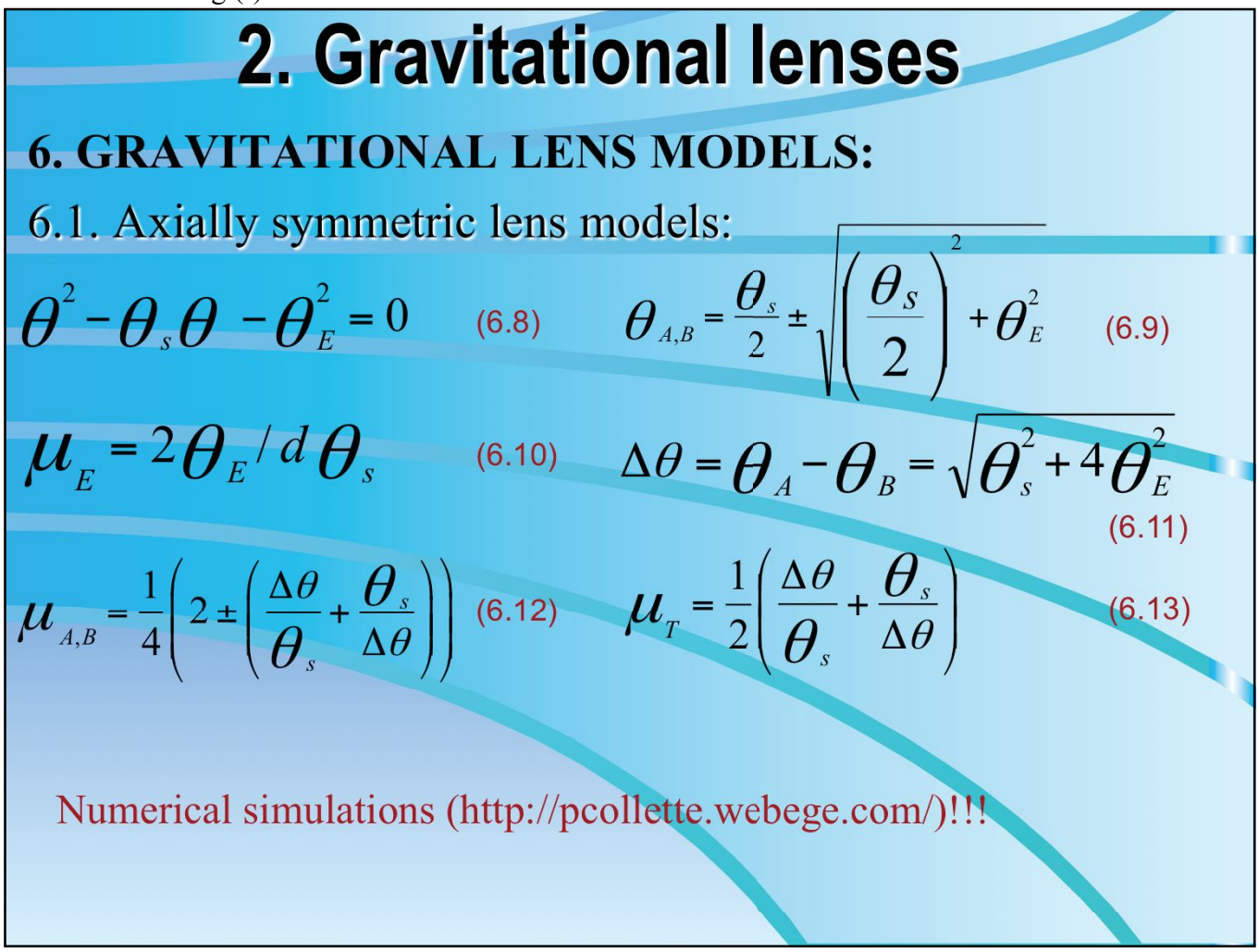

2. Gravitational Lenses:

6. GRAVITATIONAL LENS MODELS:

6.1. Axially symmetric lens models; 6.1.2. The point-mass lens model:

The total magnification (i.e. $\mu_T = \mu_A - \mu_B$) of the two images is thus

$$\mu_T = \frac{1}{2}\left(\frac{\Delta\theta}{\theta_s} + \frac{\theta_s}{\Delta\theta}\right) \qquad (6.13)$$

We can then easily deduce that for a great misalignment between the source, the lens and the observer, one of the two images approaches its true luminosity whereas the second one gets very close to the position of the deflector and becomes extremely faint. When the true position of the source lies inside the imaginary Einstein ring (i.e. $\theta_s \leq \theta_E$), the net magnification of the two images amounts to $\mu_T \geq 1.34$. This means that the cross section for significant lensing (by convention $\mu_T \geq 1.34$) is equal to $\pi\theta_E^2$, which is proportional to M (see Eq. (6.6)). We shall make use of this result when discussing the optical depth for lensing in section 7 and when using the observed frequency of multiply imaged sources within a sample of highly luminous quasars to set an upper limit on the cosmological density of compact objects in the Universe (cf. section 7.4.).

Numerical simulations (http://pcollette.webege.com/) illustrate gravitational lensing by a compact deflector.

In order to be able to see double images of a source located behind the Sun, an observer would need to go up to an heliocentric distance of 550 A.U. (the heliocentric disance of Pluto is about 40 A.U.). What would be the typical angular separation between the lensed images?

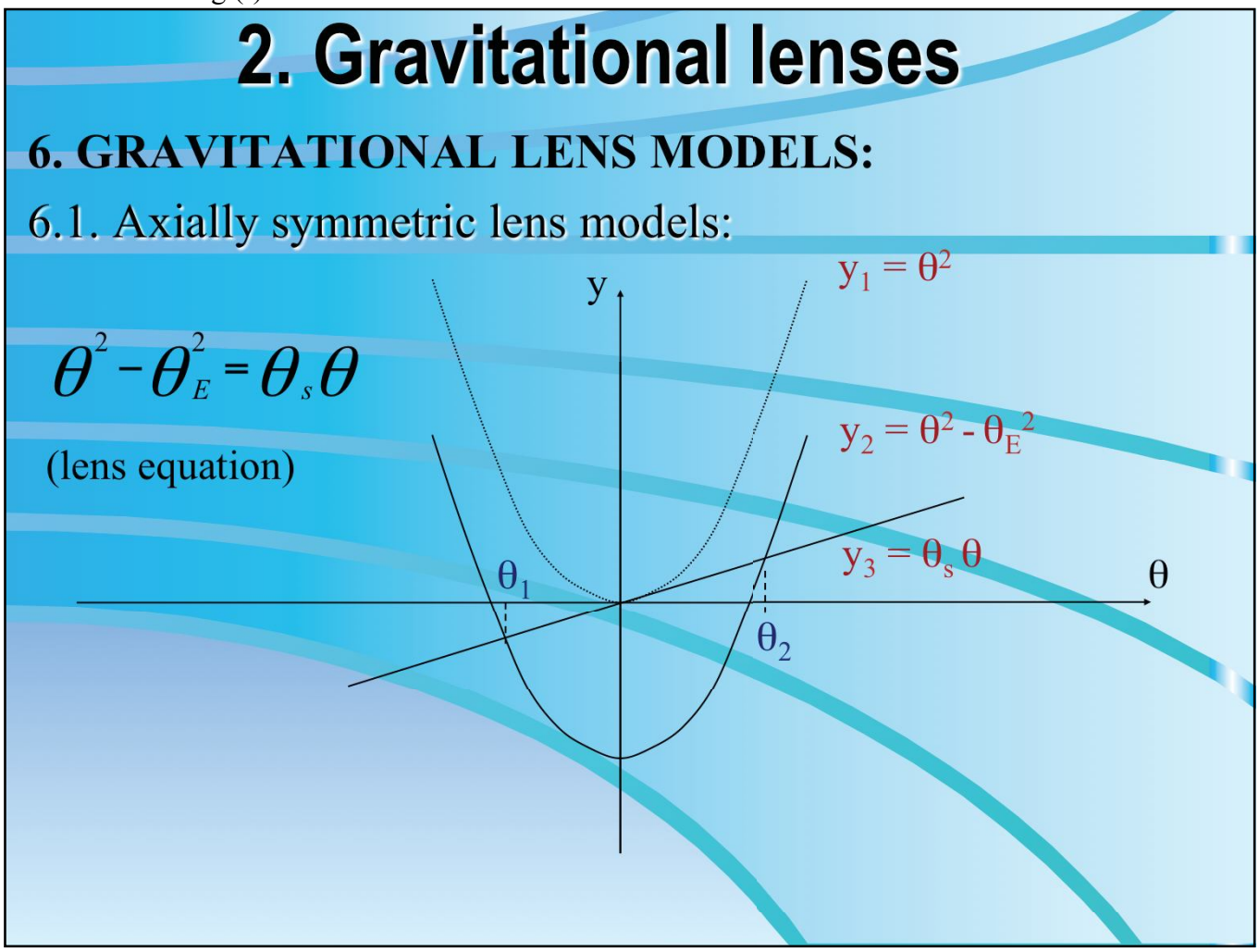

2. Gravitational Lenses:

6. GRAVITATIONAL LENS MODELS:

6.1. Axially symmetric lens models; 6.1.2. The point-mass lens model:

Another interesting graphical method to construct lensed images of a source by a point-mass lens has been suggested by Pierre Arnould. It consists in rewriting the lens equation (6.8) as indicated above. The left side of that equation represents the equation of a parabola (i.e. $y_1(\theta) = \theta^2$) that is vertically offset by θ_E^2 (i.e. $y_2(\theta) = \theta^2 - \theta_E^2$), while the right side is merely the equation of a straight line ($y_3(\theta) = \theta_s \theta$) whose slope is θ_s. The graphical solutions correspond to the two intersections (θ_1 and θ_2) between the offset parabola ($y_2(\theta)$) and the straight line ($y_3(\theta)$). It is easy to vary by $\pm d\theta_s$ the position of the source by correspondingly changing the slope of the straight line (i.e. $\theta_s \pm d\theta_s$). For $\theta_s = 0$, the graphical solutions would correspond to the positions of the Einstein ring.

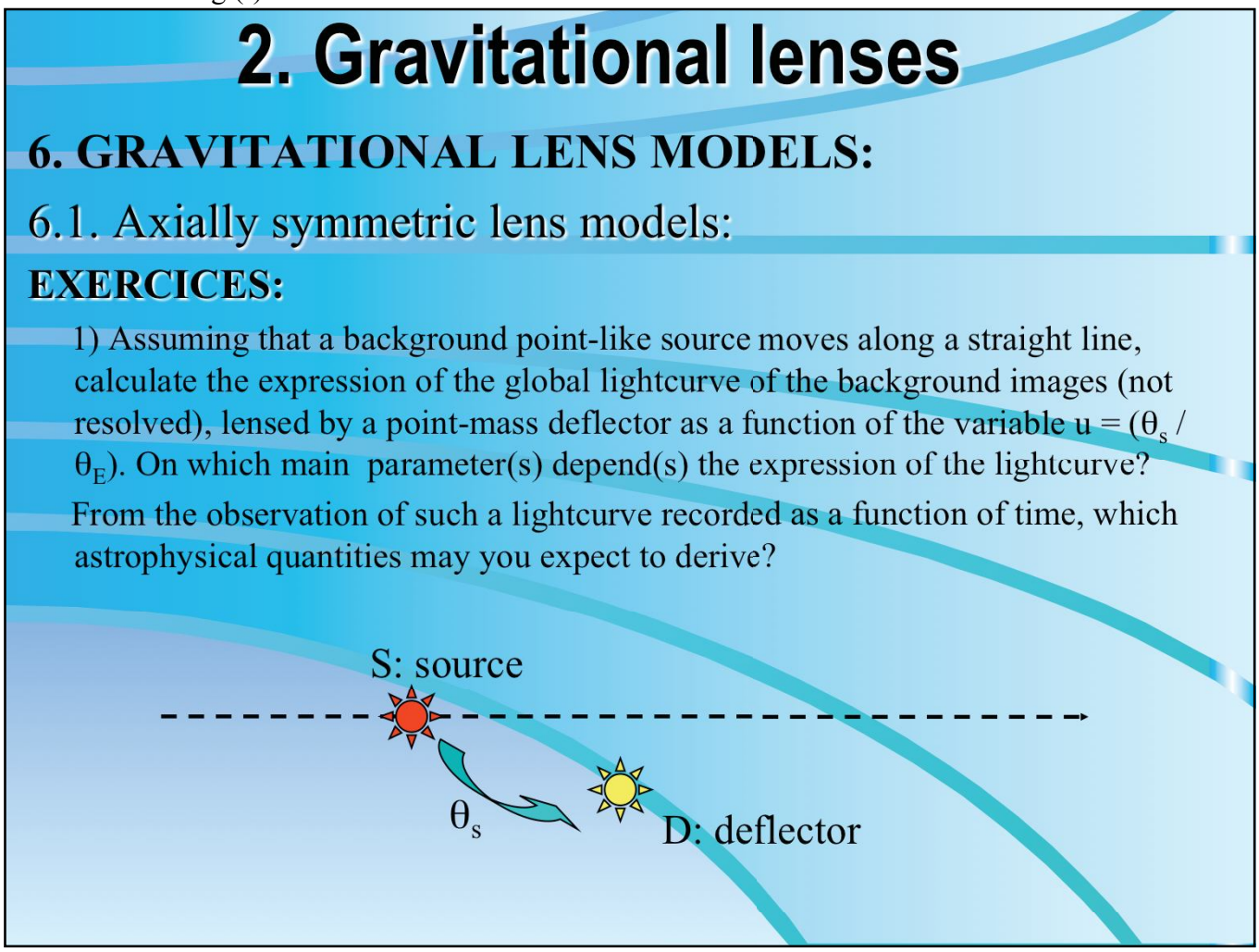

2. Gravitational Lenses:

6. GRAVITATIONAL LENS MODELS:

6.1. Axially symmetric lens models:

6.1.2. The point-mass lens model:

EXERCICES: 1) Assuming that a background point-like source moves along a straight line, calculate the expression of the global lightcurve of the background images (not resolved), lensed by a point-mass deflector as a function of the variable $u = (\theta_s / \theta_E)$. On which main parameter(s) depend(s) the expression of the lightcurve? From the observation of such a lightcurve recorded as a function of time, which astrophysical quantities may you expect to derive?

2. Gravitational lenses

6. GRAVITATIONAL LENS MODELS:

6.1. Axially symmetric lens models:

EXERCICES:

2) Show that the expression of the magnification given in (6.12) may also be expressed as (using the lens equation may prove to be very useful):

$$\mu = \frac{1}{1-\left(\theta_E / \theta\right)^4} \qquad (6.14)$$

3) Assuming that the mass distribution of the lens is of the type (cf. power law)

$$M(\theta) = M(\theta_E)\left(\frac{\theta}{\theta_E}\right)^{\beta},$$

show by means of the lens equation (4.3) that the expression of the Einstein radius θE is still given by (6.8) and that the average surface mass density Σ located inside θE is equal to the critical surface mass density Σc defined in (6.5).

2. Gravitational Lenses:

6. GRAVITATIONAL LENS MODELS:

6.1. Axially symmetric lens models:

6.1.2. The point-mass lens model:

EXERCICES:

2) Show that the expression of the magnification given in (6.12) may also be expressed as (using the lens equation may prove to be very useful):

$$\mu = \frac{1}{1-\left(\theta_E / \theta\right)^4} \qquad (6.14)$$

3) Assuming that the mass distribution of the lens is of the type (cf. power law)

$$M(\theta) = M(\theta_E)\left(\frac{\theta}{\theta_E}\right)^{\beta}$$

show by means of the lens equation (4.3) that the expression of the Einstein radius θ_E is still given by (6.8) and that the average surface mass density Σ located inside θ_E is equal to the critical surface mass density Σ_c defined in (6.5).